Assessment of early 20th Century Climate Model Simulations of Antarctic Sea Ice Using Historical Commercial Humpback Whale Catch Data

Thando Mazomba

Supervisor: Associate Professor Marcello Vichi

This dissertation is submitted in partial fulfillment for the degree of Master of Science in Applied Ocean Sciences at the University of Cape Town

December 2020

Declaration

I know the meaning of plagiarism and declare that all the work in the document, save that which is properly acknowledged, is my own. This dissertation has been submitted to the Turnitin module and I confirm that my supervisor has seen my report and any concerns revealed by such have been resolved with my supervisor.

Signed: **Signed by Candidate**
Date: December 2020

Acknowledgments

"Umntu ngumntu ngabantu." - a Nguni philosophy of Ubuntu expressed in isiXhosa, meaning "I am because you are."

I am certain that the journeys we embark on would not be possible without the people who show up to support us. This has, too, been true for me in this particular MSc academic journey.

Gratitude to my supervisor, A.prof Marcello Vichi, for his patience and understanding. Thank you for your confidence in my abilities. Thank you for sharing your knowledge and guiding me towards some of my own personal growth.

Gratitude to my family for their continued and very involved support. I never once felt I could not turn to you for anything. Thank you for your prayers, Mama noTata. Thank you for all the pep-talks, Yoza.

Gratitude to my community of friends for showing up for me constantly and in whatever way I needed.

Gratitude to my colleagues in the department for all the important conversations, the lighter conversations, the coding lessons, sharing some of your lives with me and allowing for a space of growth.

Gratitude to the Two Oceans Aquarium for giving me the opportunity to go back to studying and financially supporting me.

Gratitude to the Whales and Climate Research Program for their financial support and exposure to the type of research I wanted to step into.

Gratitude to OceanWomxn for their all-round support in celebrating and encouraging my want to step into my own. My life has changed in so many different ways because of this fellowship.

Gratitude to myself for showing up.

And from my most innate self, gratitude to the Most High.

Abstract

The story of Southern Hemisphere humpback whales through time presents multiple narratives. This study integrated two of those narratives to better understand our climate over time - the ecological behaviour of this species as well as their exploitation in the last century. The changing of our climate is largely better understood from the introduction of satellites in the late 20^{th} century, when data could be collected at higher spatial and temporal levels. Prior to this, data were scarce, especially for remote areas such as the Southern Ocean. The trust on climate models to produce valuable projections rely on how skilled they are in reproducing the historical climate; therefore their results require assessments against as many observations as possbile to further increase their reliability. The Southern Ocean being an integral component to climate regulation, it is important to try understand its oceanographic features. The seasonal sea ice cover represents one major feature of this system. This study proposes to use other sources of data for the early 20^{th} century that will help closing the gap prior to satellite observations.

Humpback whales migrate poleward during the austral summer to feed on Antarctic krill at a proximity to the ice edge. Humpback whale catch locations in the early 20^{th} century corroborate with this foraging behaviour. Using humpback whale catch location data as a benchmark, the study aims to assess the skill of climate models in simulating sea ice edge location for the early 20^{th} century. Sea ice edge is directly related to sea-ice extent, which is an important variable in the research of sea ice dynamics over time. This is especially true in the face of rapid climate change where accuracy of sea ice changes is very important. The study therefore also aims to assess climate model climatological seasonal cycle of sea ice extent results from climate models against literature and contemporary observations. Comparisons between each model's results are also carried out.

The humpback whale catch effort, as per IWC data, mostly covered the Atlantic and the Indian sector of the Southern Ocean. For this reason, the study focused on these two sectors for the analyses. Decade 1930-1939 showed the highest catch numbers consistently throughout the months of the study.

The simulated past century and recent climatological seasonal cycle sea ice extent show a wide variety of responses between the models, with the majority of them underestimating the seasonal cycle based on previous literature and contemporary observations. This indicates the need to improve the sea ice physical processes in models to better capture the specific Southern Ocean processes.The ensemble median of ice edge location from the models apparently follow the latitudinal pattern of the whale catch locations, which are assumed in this study to mark the topography of the sea ice edge. However, they simulate a sea ice edge equatorward of the edge derived from an ensemble analysis of humpback whale catch locations. The variance explained by the coefficient of determination between the models and the whale catch distribution is low, with the highest value of one month being low as well. This indicates that only a portion of the simulated edge follows the reconstructed sea ice features.

Contents

List of Figures

List of Tables

The recognition of silver linings may sometimes require a shift in perspective of the immediate narrative. This is true for the historic exploitation of humpback whale species in the Southern Ocean. With a shift in perspective, many stories are offered - of historic activities, exhibiting resilience to external forces, the successes of marine species conservation; and climate change. It is evident that one species can offer plenty to scientific research and the opportunity for cross-disciplinary scientific research. The humpback whales in the Southern Hemisphere have offered exactly that.

1 Introduction

We are observing major changes in the world's oceans that are attributed to human activities. Increasing evidence points to the anthropogenic pressures imposed on the oceans and the cryosphere. Since the pre-industrial era, the global temperature has risen by approximately 1 ^{o}C. In the framework of paleoclimatology, this rise in global temperature is a cause of major perturbations in the oceans and cryosphere (Abram et al., 2019). These perturbations have consequences for all life on Earth, including us. Marine species are already being affected by these changes (Poloczanska et al., 2013), especially those that move across larger distances, over multiple oceans, within their life cycles (Meynecke et al., 2020).

We therefore are in need of improving our understanding of the changing climate over time, to better constrain future climate responses. However, climate model simulations are not consistently reliable across the globe. In the Southern Ocean, there are major biases that affect the ability to simulate climate conditions, such as lack of observational data. This is especially apparent for Antarctic sea ice due to its inaccessibility in previous centuries(Roach et al., 2018). Species that may be more vulnerable because they have been more severely exploited can surprisingly contribute to improving the quality of climate models, especially in a period of vast Earth observation data scarcity like the early 20^{th} century.

Humpback whales in the Southern Hemisphere cover large migration distances in their life span (Rasmussen et al., 2007), from Antarctica to the continental shelves of South America and the southern regions of Africa. Because of their seasonal migrations, they may help track oceanographic features of the Southern Ocean such as the ice edge where they are known to feed, as well as coastal conditions along continental borders of the Southern Hemisphere, which are their breeding areas. Historical whaling logs provide useful insights into the Southern Ocean in the 20^{th} century, and will be used in this thesis to evaluate climate models at the beginning of the last century with a focus on the simulation of sea ice edge location.

1.1 The Importance of the Ecology of Humpback Whales

1.1.1 Humpback Whale Migration is Linked to Feeding and Calving Benefits

Humpback whales, *Megaptera novaeangliae*, are one of the marine species that migrate most extensively, making use of multiple habitats for various purposes (Stevick et al., 2011). In the Southern Hemisphere, they migrate biannually for two main purposes. The first is to calve in warmer waters during austral winters and the second reason is to feed in the Southern Ocean during austral summers (Findlay et al., 2017). This species feeds sufficiently during austral summer months to ensure enough energy storage for the long equatorward migration and calving period. Their main food source during this time is Antarctic krill, *Euphausia superba* (Surma, Pakhomov and Pitcher, 2014). Antarctic krill are present in the Southern Ocean in incredibly high concentrations during the austral summer, with the pre-rorqual-exploitation concentration standing at 25

t/km^2 (Surma, Pakhomov and Pitcher, 2014). This is due to the phytoplankton blooms that drive primary production in the region. These massive Antarctic krill concentrations sustain many secondary consumers and draw whales to the Southern Ocean during the austral summer (See Figure 1 for the Antarctic food web).

Antarctic krill are mainly distributed around the sea ice edge (Ichii, 1990), therefore it can be expected that humpback whales are also found in close proximity to the sea ice edge. This is the founding interdisciplinary basis for this study - where ecology engages with the cryosphere. The changing climate affects the Antarctic krill population size and distribution. Warming waters are not an ideal habitat for krill, forcing their distributions to move further south to more optimal water temperatures (Flores et al., 2012). Research shows that future simulations under "business as per usual" scenario project an improved growth habitat in austral spring but a worsening habitat in the austral summer and autumn (Tulloch et al., 2019; Veytia et al., 2020; Meynecke et al., 2020). The prolonged warmer sea temperatures in late summer would mean that krill abundance will decrease and their seasonal peak will shift. The phenological shift may have a cascading effect on the humpback seasonal migration and will present major consequences for the whales. With the changing climate, changes in the sea ice features (Haumann et al., 2014; Hobbs et al., 2016) may have consequences on krill distribution and therefore affect whale feeding habits. Climate models are already being used to study the projected response of whales (Tulloch et al., 2019). Understanding the possible risks that may affect whales is the reason why the thorough assessment of climate models in the Southern Ocean is important. Increasing reliability in climate models will inform us better so that we have the opportunity to take necessary interventions.

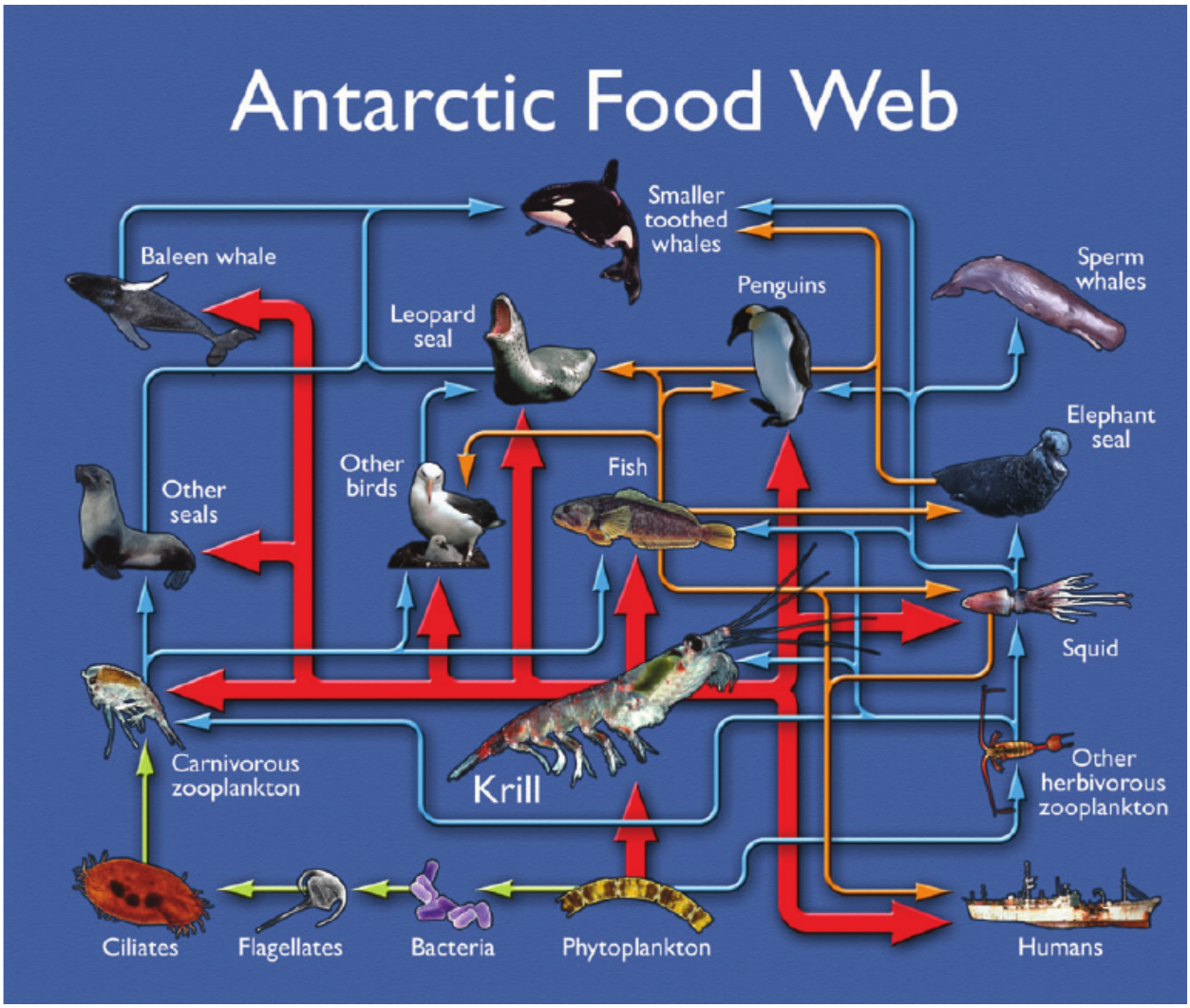

Figure 1: Antarctic food web showing the central role Antarctic krill play in sustaining many secondary consumers, including baleen whales such as humpback whales. Image sourced from McBride et al. (2014).

1.1.2 The Use of Whales in Climate Research

Whales have frequently been used in research that seeks to improve climate change understanding. Some non-exhaustive examples include Lavery et al. (2010), who investigated how iron supplementation in the iron-poor Southern Ocean via sperm whale defecation encourages the exportation of carbon to depths of the ocean for long-term storage, and Pershing et al. (2010), who researched the contribution of the ability of large whales to store carbon and sinking dead whales to sequestrate carbon, as well as how the ocean carbon cycle was impacted by commercial whaling. Ramp et al. (2015) instead analysed the shift of fin and humpback whale movements over 30 years as a result of a warming ocean. Another indirect use of whale data was proposed by de la Mare (1997), which is also the approach applied in this study. De la Mare (1997) proposed to use logbooks from commercial whaling vessels to detect Antarctic sea ice edge trends in the mid-20^{th} century. However, due to lack of data during that period and in that region, it was not a simple task. To address this challenge, de la Mare (1997) used the southern-most historical commercial whale catch logs as a proxy for the sea ice edge. The whaling records used were of a wide variety including

blue, humpback, fin, minke and sei whales. Averaging the southernmost catch latitudes collected from ship records, over October to April – the defined whaling season for this study, results showed that the summer sea-ice edge has moved southwards by 2.88 degrees of latitude between the mid 1950s and the 1970s.

De la Mare's (1997) findings were criticised for not corresponding to some sea ice extent observations, whale sightings recorded by other voyages and for unreliable data (Vaughan, 2000). De la Mare's (1997) method of using all whale species catch data was also criticised because different whale species exhibit varying behaviour and therefore hold different relationships with the sea ice edge (Ackley, 2003). Additionally, the whaling industry focused on different species at different times, creating a temporal bias in the methods (Ackley, 2003). The study was also critcised for being geographically encompassing - drawing circum-Antarctic sea ice conclusions instead of focusing on regional assessments (Cotté and Guinet, 2006). In a later paper, de la Mare (2009) showed that the historic ice charts, direct sea ice observations and whaling positions agree that a substantial southward shift in the ice-edge did occur. This paper also explained that some of the whale species are sympatric, meaning that they often feed in the same area. This therefore implies that a whaling shift in species may not have affected the results as previously argued. The paper also conducted regional analyses that spanned 220 longitudinal degrees, addressing the concern of drawing general circum-Antarctic conclusions.

Despite all the challenges in using the whale data, the appreciation of the movement of the humpback whale species through time presents an opportunity to better understand our climate. It should however be approached with caution and acknowledge the biases that are inherent to the commercial whaling practice.

1.1.3 The History of Commercial Whaling

Historically, commercial whaling has contributed to many communities and industries. The interpretation of its history depends on the recordings that have been preserved over time.

Whaling was recorded to have begun in 1000 Common Era (C.E) when the Basques began hunting Northern right whales in Bay of Biscay (whales.greenpeace.org/us). Whales were a large source of important resources, such as oil and meat. The oil, in particular, was an important contributor to the first and second industrial revolution. Humpback and sperm whales were among the main targeted species in early whaling times (WWF, 2005).

Up until the late 19^{th} century, sail boats and harpoons were the most efficient mechanisms used to hunt whales (Greenpeace, n.d). The introduction of new technology saw large-scale whaling increase rapidly. Steam boats meant that whalers could keep up with faster species, such the fin whales (WWF, 2005). Whalers could now also voyage further, for longer. The explosive harpoon, a cannon-launched harpoon that carried an explosive head, made reaching whales easier and ensured accurate and significant injury or fatality (WWF, 2005). In 1903, factory ships were built and enabled processing of killings, either in a bay or in open water (van Drimmelen, 1991). Ships with slipways at their stern made loading their kills easier and aided transport to the factory ships. The technological advancement in whaling, coupled with the increased demand for whale products during the First World War, had devastating effects on the whale populations (Smith, 1984).

Whaling in the Southern Ocean coincided with the the austral summer, poleward migration of humpback whales. Due to sea ice retreat in the summer, both whales and therefore whalers were able to get very close

to the ice edge. It was uncommon to whale in pack ice (Vaughan, 2000; Worby and Comiso, 2004; de la Mare, 2009). Vessels were not robust enough to withstand the constant impact with the ice. Maneuvering in the ice while hunting down a whale was incredibly difficult and unnecessary, especially when large amounts of whales were found at a proximity to the sea ice edge anyway.

Despite the obvious harm to marine wildlife, over-hunting whales only gained attention when oversupplying the market threatened the economic value of the industry (van Drimmelen, 1991). In 1946, the International Convention for the Regulation of Whaling (ICRW) created the International Whaling Commission (IWC) (van Drimmelen, 1991). It became the decision–making body and set a path for scientific based management of the whaling industry. The hope was to slow down whaling and conserve whale species. This was a major step in creating international accountability for whale exploitation and as a result the protection of some whale species, namely: the northern and southern right whale, the gray whale, the humpback whale, the blue whale and the sperm whale (Smith, 1984). Whale sanctuaries were also established: the Indian Ocean Sanctuary and the Southern Ocean Whale Sanctuary (IWC:Whale Sanctuaries & Marine Protected Areas, 2021[1]). The biggest achievement of the IWC, in its efforts to conserve whales, was enforcing the moratorium of all whaling as from 1986 (van Drimmelen, 1991). The difficulty in voluntary international organisations such as this is that members can be of whaling, historically-whaling or non-whaling states. It is therefore difficult to firstly pass progressive whaling laws and secondly, regulate and enforce policy. As a result, there are some countries that still carry out commercial whaling, under the objection of the moratorium, whereas the other form of whaling is subsistence whaling (Smith, 1984). The establishments of organisations such as the IWC has created a major positive shift in whaling activities (such as bans) and continues to create conversation around how people and marine life can co-exist successfully in a more sustainable manner. Some of these conversations include the implicit consequences of whaling or other activities that further apply pressure on whale populations, such as marine pollution, by-catch, whale entanglement and ship-whale collisions.

This study benefits from the IWC policy that requires all whale catches to be recorded. Catch logs consist of various information, including associated catch locations. Because humpback whales, in particular, are ecologically known to feed at a proximity to the ice edge (Andrews-Goff et al., 2018), a geographical relationship between their catch location and the location of the sea ice edge can be appreciated. The next section presents some major features of the Southern Ocean and Antarctic sea ice that will be used in the context of this thesis.

1.2 The Importance of Oceanographic Research in the Southern Ocean

1.2.1 The Biological, Oceanographic and Atmospheric Importance of Sea Ice and the Southern Ocean

Sea ice in the Southern Ocean plays a vital role in regulating the climate. It is highly dynamic, displaying behaviour that is both responsive to and a driver of the climatic conditions in the Southern Hemisphere. Sea ice trends and dynamics in the Southern Ocean directly impact ocean circulations, which play important roles in atmospheric exchanges with the ocean. This means that sea ice has the ability to influence climate conditions (Hauptmann, Gruber and Münnich, 2020).

[1] https://iwc.int/sanctuaries.

Figure 2 shows the sea ice cover from the NSIDC climatology for the months of maximum and minimum cover. Based on this figure, one can expect whale catches to occur further south during the sea ice cover minimum, in February, and closer to the equator in the austral winter.

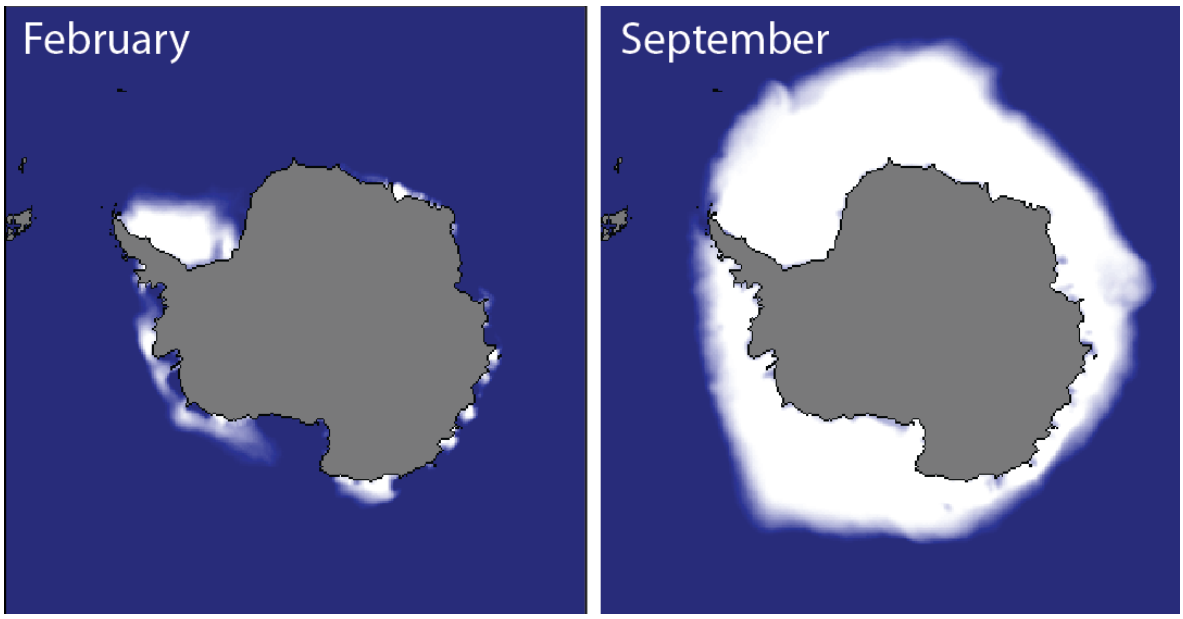

Figure 2: Antarctic sea ice cover climatology in February (minimum) and September (maximum) for period 1981 - 2010, based on passive microwave satellite data. Image courtesy of the National Snow and Ice Data Center, University of Colorado, Boulder.

Sea ice is often analysed using the measure of sea ice extent. Sea ice extent is the sum of sea ice cover per grid, based on a specific definition of what percentage of sea ice concentration (SIC) constitutes as cover. Commonly, the percentage cover is 15% SIC. It is a useful variable to use for sea ice analyses because it is spatially encompassing - it has the capacity to account for errors that may arise from small-scale features that are not always possible to resolve. In saying this, keeping the threshold of 15% SIC per grid consistent, it is possible to make comparisons of sea ice extent results between literature. Roach et al. (2020) has proposed sea ice area as a more accurate measure for sea ice, specifically because in the rapid climate change, accuracy matter now more than ever. However, keeping the threshold at 15% takes the uncertainties of remote sensing detection into account.

The climatological seasonal cycle of sea ice extent from contemporary observations, provided by the National Snow and Ice Data Center (NSIDC)[2], is shown in Figure 3. The curve shows the large annual amplitude of sea ice extent in the Antarctic, with an austral summer minimum sea ice extent of 2.5 x 10^6 km^2 and austral winter sea ice extent maximum of 19 x 10^6 km^2. The Antarctic seasonal change in sea ice extent is large and variable from year to year as indicated by the standard deviation and the record minimum and maximum in the plot. It is almost twice that of the Arctic sea ice extent seasonal change (National Snow and Ice Data Center) due to the large expanse of the Southern Ocean.

[2]https://nsidc.org/.

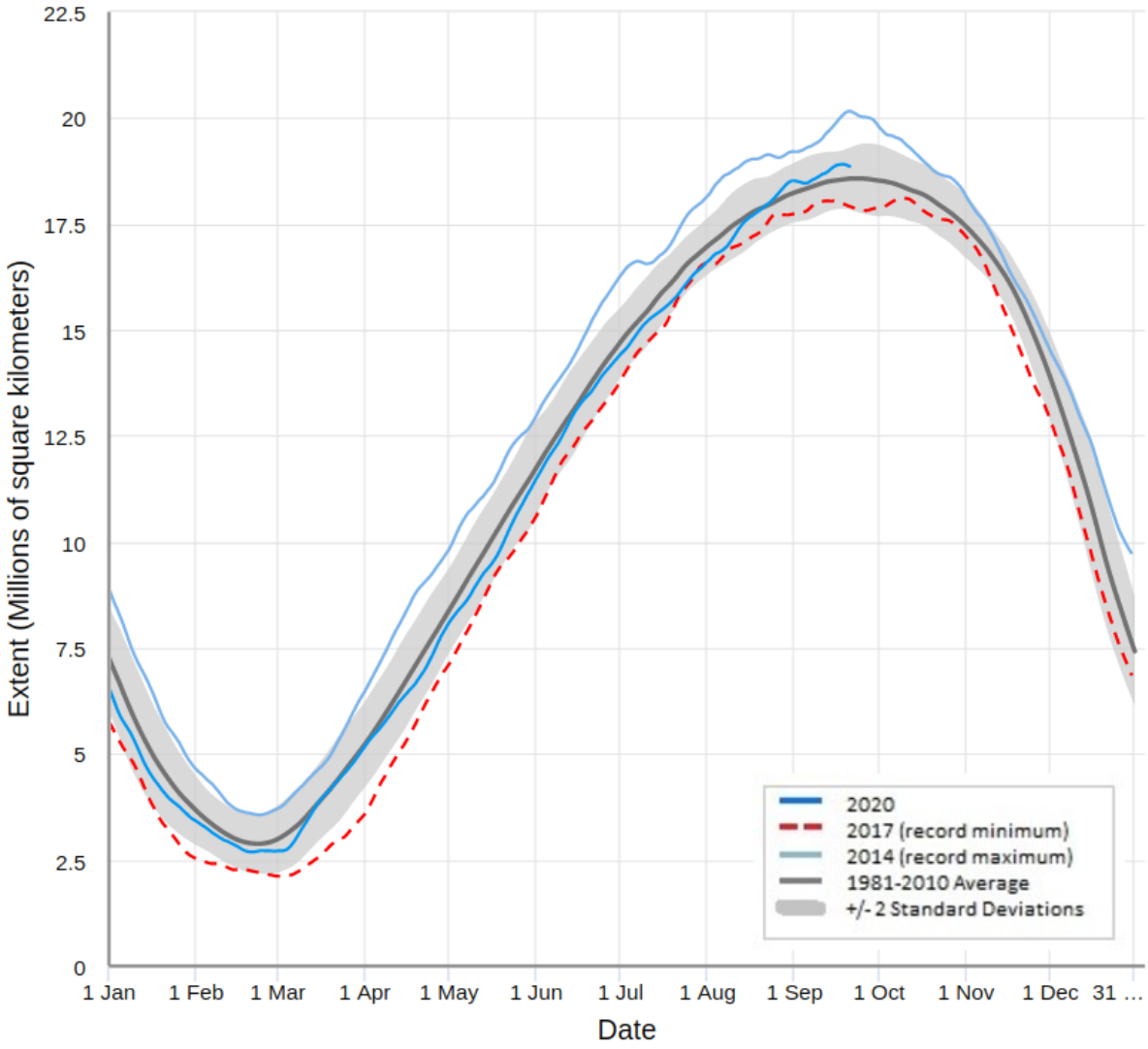

Figure 3: Climatological seasonal cycle of Antarctic sea ice extent for period 1981-2010, based on passive microwave satellite derived SIC greater than 15%. Image courtesy of the National Snow and Ice Data Center, University of Colorado, Boulder

Sea ice extent holds a close relationship with sea ice edge. Sea ice edge is the equatorward latitudinal boundary of sea ice. By convention, the sea ice edge is defined as the latitude where ice has minimum of 15% SIC. The sea ice edge identified as the 15% SIC contour line is expected to enclose the sea ice extent. Lower SIC thresholds may be used to locate the sea ice edge because although conventions are useful, they are not always the most accurate.

In the winter, the sea ice edge is often better defined than in the summer (Worby and Comiso, 2004). This is caused by the diffuse manner of the sea ice during the summer months, as the ice is often broken up and separated by water (Eayrs et al., 2019). Different types of sea ice are present in the Southern Ocean, and how they are derived, often cause sea ice edge definitions made by physical observations to differ from those made by satellites or models. For example, pack ice is usually defined as the ice edge by observers (Worby and Comiso, 2004). However, it is sometimes not signalled as such in satellites because it is unconsolidated (meaning it has water in between the ice), dynamic and subject to melt water cover (Worby and Comiso,

2004). As a result, it can be expected that physical observations of sea ice edge would tend to be more equatorward than those defined by remote sensing.

The Southern Ocean has a unique influence on climatic conditions in the Southern Hemisphere. It is geographically unique in that it is not restricted by any major land masses (Sallée, 2018). The Southern Ocean is a large area of sea temperatures capable of absorbing vast amounts of atmospheric carbon dioxide CO_2 (Talley, 2011). This makes it an important atmospheric CO_2 sink, and a vital contributor to the global heat budget. Without this important regulation, the global mean temperature would be higher than what it is now (Talley, 2011) and consequently have a major impact on human life.

Changes in atmospheric CO_2 concentrations are the main drivers of anthropogenic climate change (Abram et al., 2019). Robust atmospheric CO_2 concentration observations only began in the mid-20^{th} century (Revelle and Suess, 1957) and are now continued with several observatories around the world. Before this, observations were scarce and inconsistent. Therefore it is impossible to exactly know what the long-term atmospheric CO_2 concentrations were before then. In addition to the scarcity of observational data in the early 20^{th} century, observational data in the Southern Ocean is sparse. This is attributed to the difficulty of access to this region due to its harsh conditions and the lack of technologically advanced means to withstand these conditions (Sallée, 2018). These challenges make the reliable verification of global climate model simulations in the Southern Ocean difficult.

The relevance of this research as an interdisciplinary study

In a complex region such as the Southern Ocean, it is to our benefit to inquire many fields of research, for example the multiple Earth systems engaging one another, and how they act interdependently. Understanding climate change from multiple perspectives is critical. Research integration is essential to gain a holistic view on climate change. This is an important niche in research, not only for scientific development but because the change in climate has far reaching implications. It poses a threat to the current existence of natural environments and their ability and extent to which they can provide resources for human use. It is important to acknowledge that these implications differ in scale, depending on the risk and vulnerability of individual communities. Therefore a holistic understanding of climate change provides opportunity for more informed decision-making.

This study embodies interdisciplinary research in that it tells a circular story of the humpback whales. Using the whales to deepen our understanding of sea ice properties in the last century can only provide opportunity to better understand how our climate is changing with time. In return, improved future climate projections will equip us with information that will indicate how the future change in climate will affect the whale populations and their migratory behaviour.

1.2.2 Climate Models

What are climate models and how do they work?

Climate models are the best tool to use in holistically understanding climatic conditions with time. They simulate climatic conditions of the atmosphere, biosphere, cryosphere, hydrosphere and lithosphere in relation to how they work with one another at a global scale (Meehl et al., 2000). The term simulation

means that climate models are unable to reconstruct the exact climatic condition of a variable in a particular year or decade. They are also able to provide consistency within each simulation, which is often not possible in physical observations, since they are limited by the number of variables, the length of data capture for each variable and not having collected multiple variables for a long enough period. This becomes especially important when there is little or no data collected, particularly in the Southern Ocean.

The simulations of the physical climate are fundamentally based on physical laws that underpin the differential heating of our planet (Talley, 2011). That is, the balance of energy resulting from incoming solar radiation and outgoing radiation. All of the components that may contribute to this budget are referred to as radiative forcings constraints. Climate models simulate conditions depending on selected radiative forcings constraints and their level of influence. Figure 4 illustrates how climate models are developed and how they are used. Simulations also depend on the parameters chosen. These are mostly estimations based on calculations and literature. Parameterization is important in the processes that the climate model may not be able to resolve. Atmospheric and ocean models are dynamically coupled to include the interactive atmosphere-ocean fluxes . An example of coupled modelling is the Coupled Model Intercomparison Project (CMIP) (Meehl et al., 2000).

CMIP is an international collaboration that began in 1995, overseen by the Working Group on Coupled Modelling. CMIP aims to perform global climate analyses through the joint efforts of its constituents, in the hopes to improve climate model simulations and ultimately, the understanding of the changing climate. CMIP is now in its 6^{th} phase (CMIP6), with approximately 100 climate models from 49 modelling groups contributing, though only 40 climate models have been published thus far (Hausfather, 2019). Some of these models will contribute to the 2021 Intergovernmental Panel on Climate Change (IPCC) sixth assessment report (AR6).

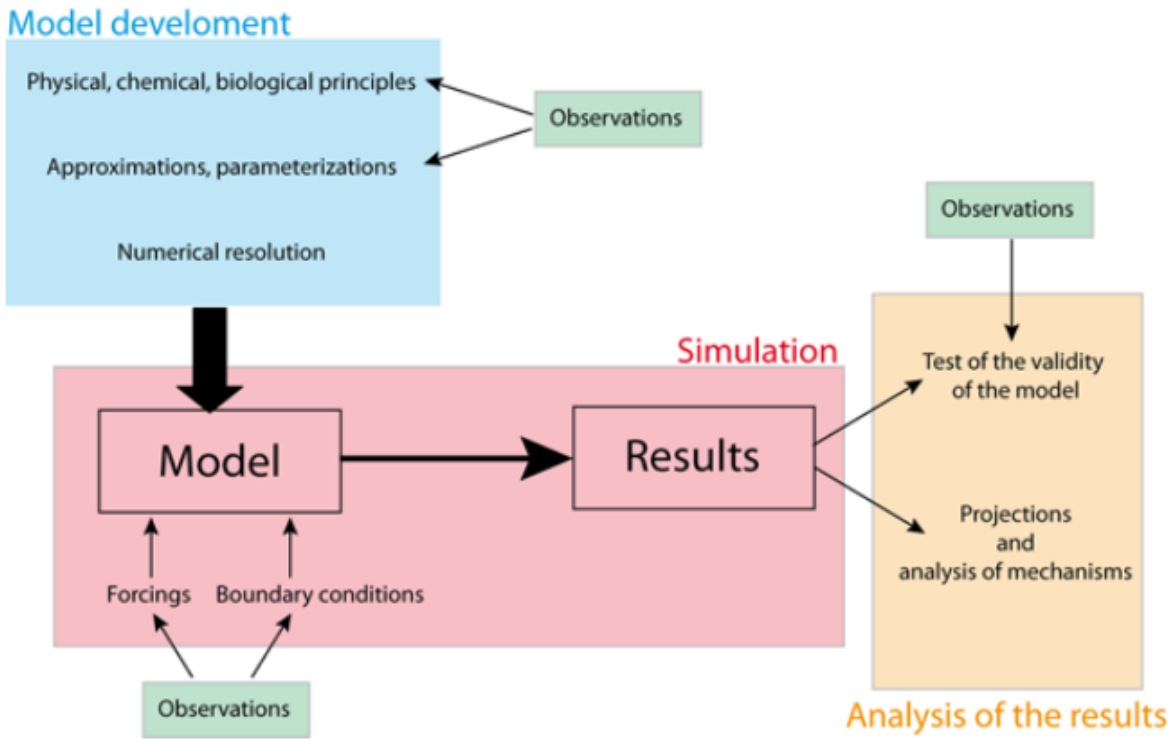

Figure 4: Diagram showing how climate models work (Goosse et al., 2010)

What challenges do climate models face in simulating Antarctic sea ice?

Climate models generally have coarser temporal and spatial resolution, which is expected since they need to be integrated for decades or centuries, as opposed to weather prediction models that are integrated for a few days at higher output frequency and require detailed topographical features. Simulations of climatic conditions must be on an inter-decadal scope in order to resolve any change in the climate. The analysis of climate simulations at scales shorter than a decade are subject to biases due to climatic internal variability that may not be the same historically recorded in the real climate. So although climate models resolve modes of variability in the Southern Annular Mode (SAM) or El-Niño Southern Oscillation (ENSO), for example, they may not be able to resolve their state in a given decade (Flato et al., 2014).

Climate models are likely to be less reliable in areas where scientific knowledge or observations are limited. As previously mentioned in Section 1.2.1, Southern Ocean observations were scarce in the early 20^{th} century. With the inability to verify climate model simulations against remote sensing observations before the last part of the 20^{th} century, we expect less confidence on the model skills to reproduce the ocean and sea ice state in the Southern Ocean in that period. The lack of observational data would require climate models to rely on parameterization validated against contemporary observations or in other regions with more abundant data, which increases uncertainty in simulation results.

The quality of climate simulations of sea ice have increased over the years, but less in the Southern Ocean. Qi Shu et al. (2020) suggest that CMIP6 models are not able to resolve the increasing sea ice extent in the Southern Ocean that contemporary observations are showing, despite its capability to capture the seasonal

cycle well. According to Zunz et al. (2013), CMIP5 faced similar challenges. The suite of CMIP6 models also underestimates the austral summer sea ice minima (Roach et al., 2020) as done in the two previous cycles (CMIP3 and CMIP5). These results may be due to CMIP6 inability of capturing the high Antarctic sea ice extent interannual variability which likely affects how well models can simulate climatic trends (Qi Shu et al., 2020; Roach et al., 2020). Furthermore, this may be due to global climate models being challenged with resolving zonal atmospheric features at a regional scale (Hobbs et al., 2016). Zonal atmospheric features such as winds are important to resolve as they majorly influence the behaviour of sea ice in the Southern Ocean.

CMIP6 sea ice extent biases against contemporary observations, show an increase from its predecessor, CMIP5 (Qi Shu et al., 2020). There is general uncertainty on how to capture trends in global climate models because of the short time frame of contemporary remote sensing - meaning that with only a 40 year consistent record, features could arise from any type of variability (Maksym, 2019). Figure 5 shows how projected climate model trends of annual seasonally-averaged sea ice extent differ between austral seasons, and how they compare to contemporary satellite and proxy observations.

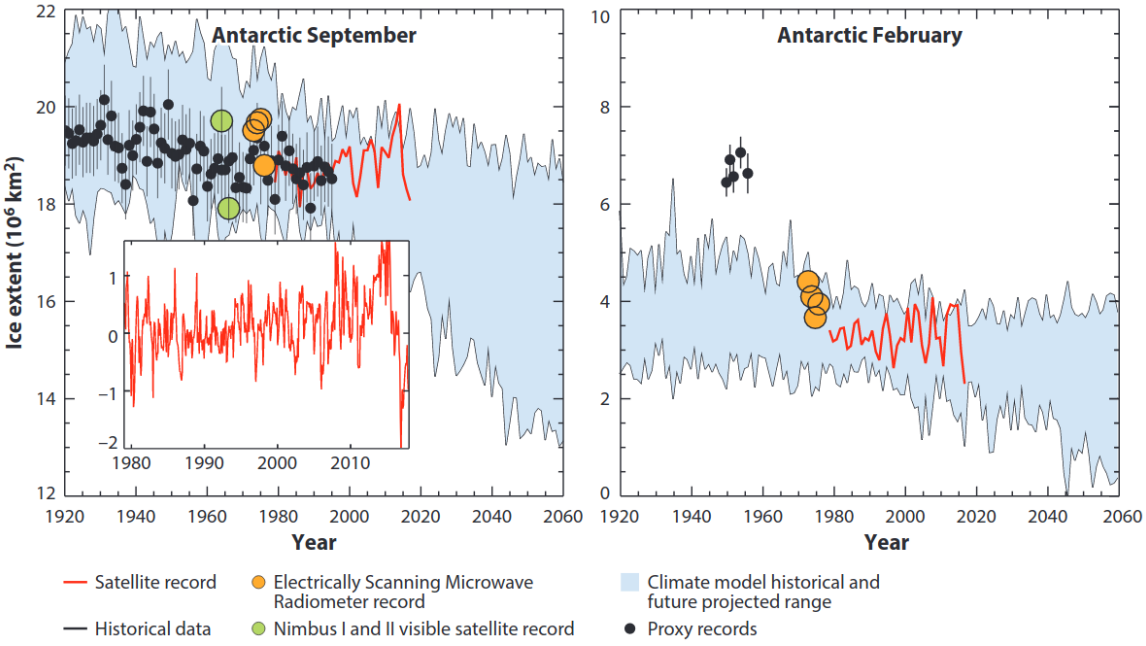

Figure 5: Annual Antarctic sea ice extent output averaged over austral winter months (left panel) and summer (right panel) from different sources.

Considering all these challenges, assessment of climate model results is an important exercise because it provides opportunity to determine where climate models are doing well and where they need evaluating. This is especially important for regions lacking in data and even more so when they are a significant contributor to the climate, such as the Southern Ocean.

1.3 Research Aims and Objectives

Climate models are the only tool for producing future projections, but their reliability depends on the capacity to simulate historical climate conditions. Their improvement thus depends on constant assessment of their results. One of the ways this can be achieved is through the assessment against observational data, which is currently being enhanced by the availability of Earth observation data through satellites.

The limitations in reconstructing early 20^{th} century conditions, as a result of sparse in situ data (see Section 1.2.2) prevent an accurate simulation of Antarctic sea ice properties. The use of humpback whale catch data presents an opportunity to fill some of these data gaps. This study will therefore use the whale catch data as a representative of a **pre-Earth observation era**.

Although the number of Earth observations began to increase since the International Geophysical Year in 1957-58 (Baird, 2014), spatially and temporally robust observations came only with the introduction of satellite observations, since 1979. In this thesis, the period covered by satellite data is representative of an **Earth observation era**.

The significance of this is that climate model results of Antarctic sea ice features can be assessed in two different periods: the pre-Earth observation and the Earth observation eras. The longer term aim is that more accurate historical simulations will lead to more reliable projections, allowing us to make better informed decisions with regards to taking appropriate measures for both the changes in the climate and its effect on natural ecosystems. This work is organized around the aims and specific objectives listed in the following two sections.

1.3.1 Aims

1. The study aims to assess the performance of Antarctic sea ice simulations from CMIP6 climate models in the early 20^{th}century. The focus will be on the spring-summer location of the sea-ice edge that will be compared against historical humpback whale catch location data.

2. The study will also analyse the results of sea ice seasonal cycle simulations in the Southern Ocean by contrasting the pre-Earth observation era with the Earth observation era. This aim will focus on the sea ice extent, which is the key variable obtained through satellite data.

1.3.2 Objectives

- Pre-Earth observation era climate model results of sea ice edge, will be synthesized to produce results which will be assessed against humpback whale catch location results. This swill determine the performance of climate model sea ice edge simulations during the period and in the region of available whale observations.

- These results will be contrasted with the sea-ice simulation results for other periods to check for changes in the simulated features during the pre-Earth observation era.

- The climatological seasonal cycle of sea ice extent for each climate model will be calculated for the pre-Earth observation era and the Earth observation era. For both eras, it is important to compare results produced by different models. For the observation era, the simulated sea-ice seasonal cycle will be assessed against the satellite climate data record to class the performance of each of the models.

- A climate model comparison of the annual summer mean time series of sea ice extent for pre-Earth observation and Earth observation era will be carried out to see if there are differences in results between the two eras.

2 Methodology

This section is split into the two subsections, namely 2.1) Data Sources and 2.2) Variables used as Benchmarks and Indicators. The indicators describe the objectives mentioned in Section 1.3.2.

2.1 Data Sources

2.1.1 Whale Data

The historical commercial whale catch data were sourced from the unpublished latest version of the catch database from the IWC, courtesy of Cherry Allison from the International Whaling Commission, Cambridge, UK. The preparation of the data was conducted by Dr Elisa Seyboth, from the Cape Peninsula University of Technology, South Africa. Because this study focuses particularly on humpback whale catch locations, the preparation included filtering the data for humpback whale catches only. It also included regridding the data to a 10 x 10 degree resolution and categorization of whaling operation based vessel logbooks. A summary of the categorization of whaling operation is described in Table 1 1. In the Southern Hemisphere, a total of 215928 humpback whale catches were logged between the period 1890 and 1978. The logs ranged all the months of each year in this period. Figure 6 shows the spatial distribution of the catch logs during this period.

Humpback whale data biases

It is important to acknowledge the limitations the humpback whale catch data present. Historical commercial whaling vessels were technologically basic and therefore voyages were only possible weather permitting, presenting a temporal bias in data. The lack of technological advances in vessels also limited the voyages spatially. Additionally, whalers voyaged with the objective of whaling and therefore voyaged to areas known to inhabit whales. As a result, records followed a presence-only model. However, as mentioned in Section 1.1.3, it was not common for whalers to hunt in the ice, therefore this presence-only model is controlled only by the latitude of the logged catch, and represents a northernmost limit of the ice edge location at the time of the catch.

The catch logs were also reliant on what was logged - all illegal and non-logged catches were not included in the data. Despite the limitations within the data, the large catch numbers have allowed for a robust sample size.

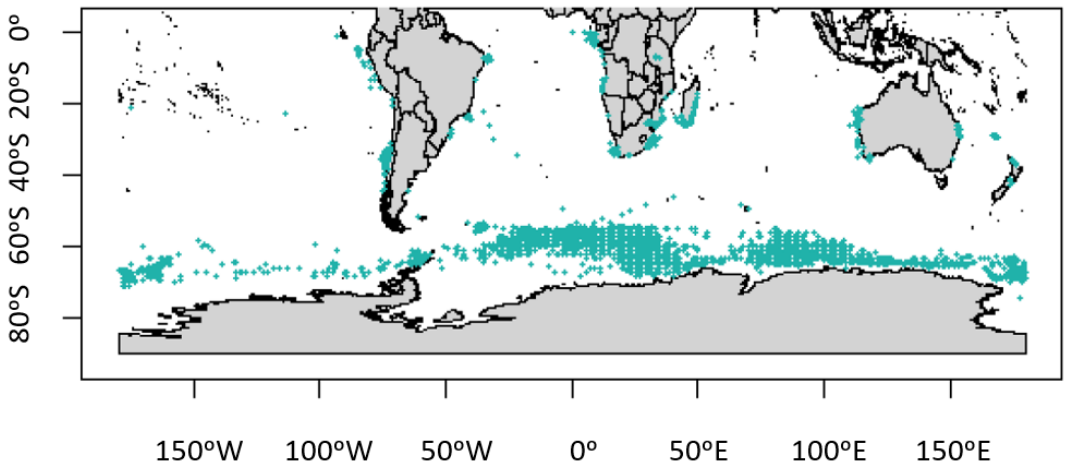

Figure 6: Humpback whale catch distribution recorded between 1890 and 1978 in the Southern Hemisphere, as per IWC records. Image is courtesy of Dr. Elisa Seyboth, Cape Peninsula University of Technology.

Table 1: Types of whaling operations carried out in the Southern Ocean in the last century, as per IWC records. Information is courtesy of Dr. Elisa Seyboth, Cape Peninsula University of Technology.

Type	Description
Individual	Individually logged catches with individual corresponding coordinates
Small Area	Logged catches in a small area around the anchor of the floating factory(ship), at noon, corresponding with one common coordinate
Whaling Station	Logged catches corresponding to the coordinates of the mother ship whaling station
Broad Area	Logged catches in a large area around the anchor of the floating factory(ship), at noon, corresponding with one common coordinate

2.1.2 Climate Model Data

This study made use of data produced by models that contribute to CMIP6 and were available at the time of the analysis (November 2019). The data were sourced from Earth Systems Grid Federation (ESGF), an open source online platform for climate model data [3]. The main model output used in the study was SIC, which was downloaded for all the selected models for the period 1900-2015. The grid cell area was also collected.

Models were initially selected based on the following parameters (See Table 2). The Variable parameter is a basic variable selection, where *siconc* is the state variable, SIC; and *areacello* is the ocean grid cell area. The grid cell area files carried the same resolution as their state variable counterparts and both files were compliant with CF-1.7CMIP-6.2.[4]Both outputs shared the same Experiment ID, Grid Label and Variant

[3]https://esgf-node.llnl.gov/projects/cmip6/
[4]https://docs.google.com/document/d/1os9rZ11U0ajY7F8FWtgU4B49KcB59aFlBVGfLC4ahXs/edit [draft in session].

Label. The Experiment ID is the root experiment identifier. The historical experiment, temporally ranging from 1850 to 2014 for CMIP6, is chosen based on the analysis period for the study. The Grid Label allows for the selection of grid types. The native grid selected for the study, abbreviated "gn", is the primary grid where no regridding procedure has been conducted. The Variant Label describes the individual ensemble member simulation, using the "rip" nomenclature to allow for selection: r describes the initial state or the realization of the member, i describes the initialization; and p for the physics used. If a forcing is used in the simulation, f is added into the nomenclature. The integer used within the nomenclature describes the run which follows a specific protocol within CMIP6. Ensembles were not used in this study, which focused on inter-model differences, and thus the first reference run was used for each model. The two model variables differ in their Frequency and Table ID. The Frequency describes the sampling frequency, where monthly is selected in the SIC output and fixed is selected for the grid cell area output. The Table ID assists in identifying the sampling frequency, for example if the sampling is carried out monthly or it is a fixed variable.

Table 2: The six main parameters on the CMIP6 search interface on the ESGF online platform used to obtain the climate models, and the available SIC grid cell area files, used in the study.

Parameters	Parameters Chosen (siconc)	Parameters Chosen (areacello)
Variable	siconc	areacello
Experiment ID	historical	historical
Grid Label	gn	gn
Variant Label	r1i1p1f1	r1i1p1f1
Frequency	mon	fx
Table ID	Omon	Ofx

A total of 23 model outputs of SIC and 17 grid cell area model outputs were downloaded, based on availability for download at the time. Table 3 expands on the description of the models downloaded.

Table 3: A description of the 23 climate models used in the study and the availability of their SIC grid cell area file counterparts.

Model	Institution	Resolution (km)	References	Grid Cell Area File
ACCESS-CM2	Commonwealth Scientific and Industrial Research Organisation	250	Dix et al., 2019	yes
ACCESS-ESM1-5	Commonwealth Scientific and Industrial Research Organisation	250	Ziehn et al., 2019	yes
CAMS-CSM1-0	Chinese Academy of Meteorological Sciences	100	Rong, 2019	no
CanESM5	Canadian Centre for Climate Modeling and Analysis	100	Swart et al., 2019	yes
CESM2	National Center for Atmospheric Research	100	Danabasoglu,2019	yes
CESM2-WACCM	National Center for Atmospheric Research	100	Danabasoglu,2019	no
EC_Earth3	EC-Earth-Consortium	100	EC-Earth Consortium (EC-Earth), 2019	yes
FGOALS-f3-L	Chinese Academy of Sciences	100	YU, 2019; He et al., 2020	yes
FGOALS-g3	Chinese Academy of Sciences	100	Li, 2019	no
FIO-ESM1-0	First Institute of Oceanography	100	Song et al.,2019	no
GFDL-CM4	Geophysical Fluid Dynamics Laboratory of The National Oceanic and Atmospheric Administration	25	Guo et al., 2018; Adcroft, et al., 2019	no
GFDL-ESM4	Geophysical Fluid Dynamics Laboratory of The National Oceanic and Atmospheric Administration	50	Krasting et al., 2018; Held et al., 2019	yes
IPSL-CM6A-LR	Institut Pierre-Simon Laplace	100	Boucher et al., 2018	yes
MIROC6	Atmosphere and Ocean Research Institute (The University of Tokyo),National Institute for Environmental Studies, and Japan Agency for Marine-Earth Science and Technology	100	Tatebe and Watanabe, 2018	yes
MPI-ESM-1-2-HAM	Max Planck Institute HAMMOZ-Consortium	250	Neubauer et al., 2019	yes
MPI-ESM-1-2-HR	Max Planck Institute	50	Jungclaus et al., 2019; Mauritsen et al., 2019	yes
MPI-ESM-1-2-LR	Max Planck Institute	250	Wieners et al., 2019; Mauritsen et al., 2019	yes
MRI-ESM2-0	Meteorological Research Institute	100	Yukimoto et al., 2019	yes
NorCPM1	Norwegian Climate Prediction Model	100	Bethke et al., 2019	yes
NorESM2-LM	Norwegian Climate Services Centre	100	Seland et al., 2020	yes
NorESM2-MM	Norwegian Climate Services Centre	100	Bentsen et al., 2020	yes
SAM0-UNICON	Seoul National University	100	Park et al., 2019	yes
Tai ESM1	Research Center for Environmental Changes, Academia Sinica	100	Lee and Liang, 2020	no

2.1.3 Satellite Data

The contemporary observations in the study were represented by data of SIC derived from global passive microwave, sourced from the European Space Agency (ESA), specifically their Climate Change Initiative's (CCI) Sea Ice Concentration Climate Data Record (CDR).[5] The data were generated by the European Organization for the Exploitation of Meteorological Satellites (EUMETSAT) Ocean and Sea Ice Satellite Application Facility (OSI SAF), computing SIC from brightness temperatures picked up by the following sensors: Scanning Multichannel Microwave Radiometer (SMMR), Special Sensor Microwave/Imager (SSM/I) and Special Sensor Microwave Imager/Sounder (SSMIS) - a polar orbiting radiometer (Lavergne et al., 2019). The sensors are situated on Nimbus-7 and Defense Meteorological Satellite Program (DMSP) platforms (Tonboe et al., 2017), the latter specifically pertaining to the DMSP-F<08,10,11,13,14,15 and the DMSP-F<16,17,18 platforms. The data have a frequency of bi-daily records (every 2 days) up until the mid 80's, and from then onward were daily records. The spatial resolution of the data is 25 km. The observations downloaded span years 1979, the commencement of the satellite era, to 2014. The metadata were compliant with CF-1.6 ACDD-1.3. [6]

2.2 Variables Used as Benchmarks and Indicators

To understand climate model results in the Southern Ocean, two indicator variables were used. These indicator variables were used to either assess climate model results against benchmark variables and/or compare results between models. Benchmark variables are variables from observational data, therefore carrying high reliability. All variables have been derived from whale, climate model and satellite data.

2.2.1 Benchmark Variables

Humpback whale catch distribution

As mentioned in Section 1.1.3, whaling in the Southern Ocean took place in the austral summer, which is typically December through to February. To take advantage of large catch numbers during this season, this study focuses its analyses in these months, with an addition of the late spring November month. Including November increases the study's sample size and the temporal and spatial context of the distribution of the whale catches.

The whale catch data were filtered for catches from 40^oS, poleward. Only the data with a reported location were used. These could either be exact, approximated or the mother ship locations. The whale catch location data were reorganised, from Figure 6, to show the spatial and temporal distribution in catch locations in each selected month, and for each decade in the early 20^{th} century. Decades are indicated by the central year of the period, such as the decade 1930-1939 is labeled 1935, and so on. A decade is a sufficiently long period to gain statistical significance in the catch size and to smooth out year to year variability. Whaling rapidly decreased after the 1950s with the establishment of the ICRW in 1946 and due to the crash in whale populations, resulting in very low catch records after that. A complementary tallying of decadal catches, in each of the selected months was carried out. Similarly, this was carried out for an annual

[5] https://osisaf-hl.met.no/osi-450-430-b-desc.

[6] `https://osisaf-hl.met.no/sites/osisaf-hl.met.no/files/user_manuals/osisaf_cdop3_ss2_pum_sea-ice-conc-climate-data-record_v2p0.pdf`.

analysis. A selection of a decade with the best spatial and temporal coverage of whale catches was made and selected as the reference decade to compare with the corresponding climate model simulations. The possible inter-decadal variability of the simulated climate will be taken into account in the result section.

Whale catch data are uncertain in their exact location but do represent real physical observations. They therefore carry a good level of reliability, making them a strong benchmark against which to assess climate model sea ice edge results.

A statistical latitudinal distribution of the whale catches was computed per 10 degrees longitude to show the central tendency of the catches, latitudinally. This will allow for the climate model sea ice edge results to be compared against the latitudinal bulk of the catch data. The 10 degrees longitudinal stratification enables a geographical breakdown of the whale catches to allow for regional assessments. For the distribution to be most telling, sample sizes per longitudinal group would need to be at least 5 records (Krzywinski and Altman, 2014). Therefore in longitudinal groups with less than 5 whale catch records, interpreting results may be limited.

Contemporary satellite data

The satellite data pre-processing was done through Climate Data Operators (CDO) software, version 1.9.3[7]. It included the concatenation of all observations per year and subsequently the concatenation of all years. A climatological monthly mean and standard deviation was then calculated for the period for the entire Antarctic sea ice extent.

2.2.2 Climate Model Assessment and Comparison Indicator: Sea Ice Extent

Sea ice extent is the sum of sea ice covered grid cells, based on a specific definition of what percentage of SIC constitutes a covered grid cell. Commonly, the percentage cover is 15% SIC, which means that a cell with more than 15% SIC is assumed fully covered. This is different from sea ice area, which is the total area of the ice-covered ocean. Sea ice extent was used as an indicator through assessing the monthly time series of sea ice extent for the last century, for each model. Additionally, assessments of the climatological seasonal cycle of sea ice extent, for the observation era, for each model were made against contemporary satellite observations provided by ESA CCI Sea Ice Concentration CDR (See Section 2.1.3). Sea ice extent was used as a comparison indicator through comparing the climatological seasonal cycle of sea ice extent results between models, for both the pre-Earth observation and observation era. With sea ice extent being an encompassing variable, it is expected that climate models capture it relatively well. Using this variable, climate models were classed based on their ability to capture the seasonal cycle of sea ice extent.

Pre-processing the climate model data was done through the CDO software version 1.9.6.[8] It included selecting the time period 1900-2014 per model. Only 17 grid cell area files were available at the time of downloading (See Table 3) therefore only 17 climate models were used to compute this assessment indicator. Some of the model data uploaded on the ESGF platform contained errors as a result of missing metadata, lacked correspondence between the geometry of the grid cell area and the state variable files; and missing values on land that were not properly identified. To avoid reducing the number of files available to this study, these data were manually corrected. This included latitudinal reorientation and excessively-large

[7] http://mpimet.mpg.de/cdo.
[8] http://mpimet.mpg.de/cdo

number replacements for FGOALS-f3-L and replacing state variable coordinates with the grid cell area file coordinates for models ACCESS-CM2, ACCESS-ESM1-5, CanESM5, CESM2, EC_Earth3, GFDL-ESM4, IPSL-CM6A-LR, MIROC6, MPI-ESM-1-2-HAM, MPI-ESM-1-2-HR, MPI-ESM-1-2-LR, MRI-ESM2-0, NorCPM1, NorESM2-LM, NorESM2-MM, SAM0-UNICON and FGOALS-f3-L .

Computation

The Antarctic sea ice extent *SIE* was first computed for the period 1900-2014, based on the following formula:

$$SIE = \sum_{i=1}^{N} A_i \left(SIC_i > 15\%\right)$$

where i is the grid element index, up to the total number of grid points N, A_i is the grid cell area and SIC_i is the ice cover at that grid point for each month.

A monthly time series, for the previous century, of sea ice extent measurements for each model were carried out. The climatological seasonal cycles of SIE were then calculated both for the pre-Earth observation and the Earth observation reference periods.

For observation era, it was used to assess climate model results against the benchmark of contemporary satellite observations described in Section 2.1.3. Models were then classified based on the proximity of their results of sea ice extent seasonal cycle to that of the satellite observations, using the mean bias computed for each model:

$$\overline{B}^{mod} = \frac{1}{12} \sum_{n=1}^{12} SIE_n^{mod} - SIE_n^{obs}$$

where the index n runs over the climatological monthly value.

The threshold used to distinguish the 1^{st} -rated models was a difference value of 0.86 x 10^6 km^{6}or less. Second-rated climate models were also selected as the next class of models with the next-closest curves to that of the satellite. The threshold used to distinguish the rest of the models from the 2^{nd} -rated models was a difference value of 3.5 x 10^6 km^{6}or greater.

2.2.3 Climate Model Assessment Indicator: Sea Ice Edge

Sea ice edge is the equatorward latitudinal boundary of sea ice. This variable is useful due to the geographical and ecological relationship it has with humpback whale feeding behaviour. It will allow for the assessment of climate model sea ice edge results against benchmark of the latitudinal distribution of whale catch location data.

The same pre-processed SIC data from the previous section were used. In this case however, each selected month as defined in the study (November, December, January, February), was extracted per year, for the temporal scope of the study, 1900 - 2014.

Computation

The sea ice edge location was computed for each selected month of the study, per model. The data were restricted to a latitudinal minimal threshold of 40^{o}S. The sea ice edge location in model output was

computed based on a SIC value greater than 0%. Most research (for example, Comiso et al., 2020) uses a common minimum threshold of 15% SIC detection, reason being that a SIC detection below 15% SIC from satellites begins to carry uncertainty. However, since this variable is here compared with the location of whale data that were most likely in open ocean, a more conservative threshold of 0% is preferable.

The CMIP6 data uploaded by the individual teams were not all configured to a common indexing, specifically for the longitude coordinates. This therefore required rolling the longitudinal axes to a common index. Most of the models carried a latitudinal dimension size of 360, therefore regridding onto a common grid of 0^o - 360^o by 0.5 degree intervals, was carried out. In accordance with the whale data, decadal means were calculated, per individual model, for the initial analysis period, 1900-2014, for each selected month. A statistical distribution of the models for the ice edge location was then computed, both for the best models and for the second rated models.

Distributions of the median sea-ice edge location and the inter-quartile ranges were compared against the benchmark of whale catch distribution, for each of the selected months. These were done by superimposing the climate model distribution onto the whale catch location distribution.

3 Results

3.1 Humpback Whale Catch Distribution

The re-organised distribution of the whale catches per decade obtained from the IWC database (Section 2.1.1) is presented in Figure 7 using both a Mercator and stereographic projections.

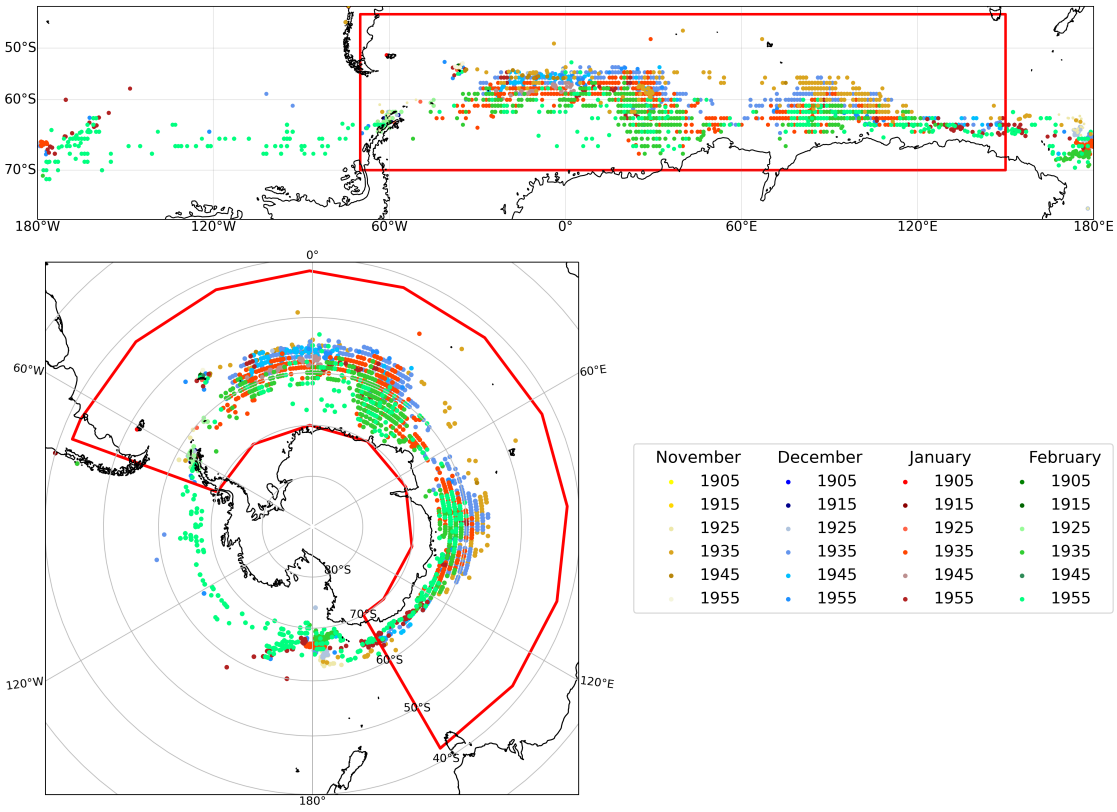

Figure 7: Decadal distribution of humpback whale catches recorded between 1900 and 1978 in the Southern Ocean, for each month in the study. Decades are labeled by the middle year. The red box indicates the area of focus in the study - the Atlantic and Indian sector of the Southern Ocean. See Table 4 for the number of catches in each cluster.

This visualisation improves the understanding of the distribution of catches from Figure 6 presented in the Section 2 by showing the stratification by decade and month. As explained in the methodology, the decade is identified by the middle year (e.g. 1915 identifies the decade 1910-1919) and the selected months cover the late spring-summer period, from November to February. The distribution of whale catches for the last century are spatially condensed in the Atlantic and Indian sector of the Southern Ocean. The lack of data in the Pacific sector makes it unfavourable to carry out assessments within this sector. The analysis will therefore focus in the Atlantic and Indian sectors of the Southern Ocean.

Figure 7 shows a poleward movement of catches with the progression of the summer season (from the yellow to the green hues). This indicates the whalers followed the whales further south as the sea ice retreated over time. This visually shows and supports the known behavioural ecology of humpback whales (Section 1.1.1 and 1.1.3), which feed in the proximity of the sea ice edge.

Table 4 and Figure 8 report the number of whale catches for each month of the study for each decade in the last century. Catches within each month show an increase from the start of 20^{th} century, peaking in the decade 1930-1939, before starting to decline towards the middle of the century. Within each decade, maximum catch records were recorded in either December or January, with the exception of the maximum catch recorded in February in the decade 1950-1959.

Table 4: Decadal humpback whale catches in the last century for each month of this study. Catches are binned in the center of each decade.

Decade	Month			
	NOVEMBER	DECEMBER	JANUARY	FEBRUARY
1905	0	179	1	0
1915	583	672	694	154
1925	199	555	897	379
1935	1038	5088	4873	3166
1945	77	1939	209	11
1955	9	382	2701	10066

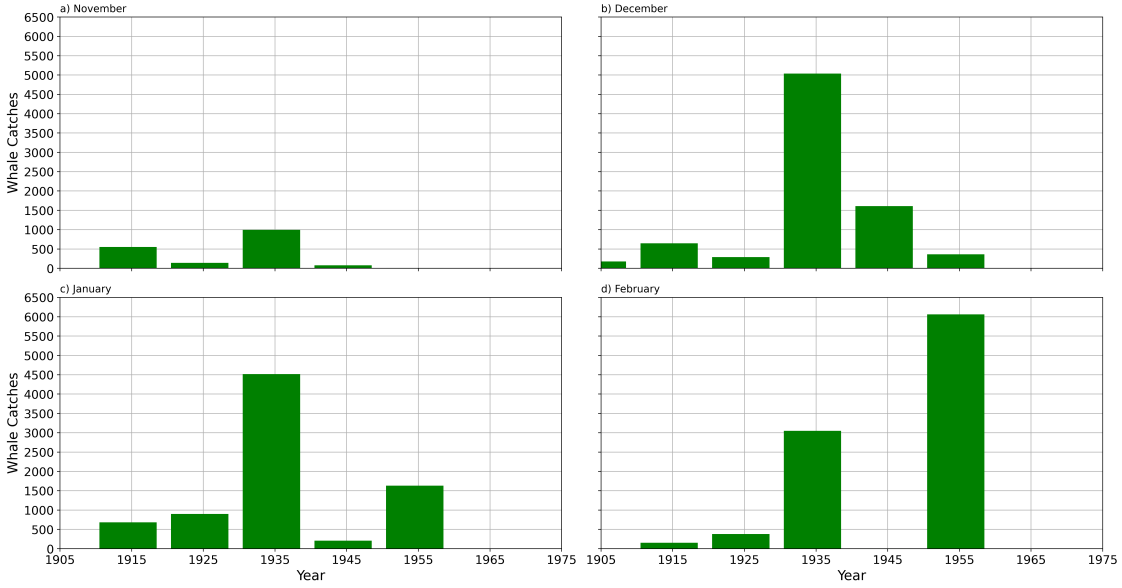

Figure 8: Humpback whale catches recorded per decade for a) November, b) December, c) January and d) February. Bins are centered in the middle of the decade. For example, the label 1915 represents the decade 1910 - 1919.

The decade 1950-1959 shows the largest number of catches in the month of February. This number contrasts with the catches observed in February in all the other decades. This abrupt increase in humpback whale catches in the 1950s has been attributed to the illegal whaling conducted by the Union of Soviet Socialist Republics (USSR) as reported by Walsh (1999). Because these high catches are not consistently seen in all four months, this decade would represent a biased benchmark. Decade 1930-1939 however shows

high catch numbers consistently throughout all four months. This decade has the best spatial and temporal distribution of whale catches, as aimed for in Section 2.2.1. It has therefore been chosen as the reference period for the pre-Earth observation era.

3.2 Early 20^{th} Century Sea Ice Extent Features

The simulated climatological seasonal cycle of sea ice extent, for the entire Antarctic, from the chosen decade representing the pre-Earth observation era is presented in Figure 9. In addition to analysing the climatology over the reference period, a monthly time series of sea ice extent measurements produced by each model, for the 20^{th}century, was carried out. This result is shown in Appendix B, with Figures 15 to 31.

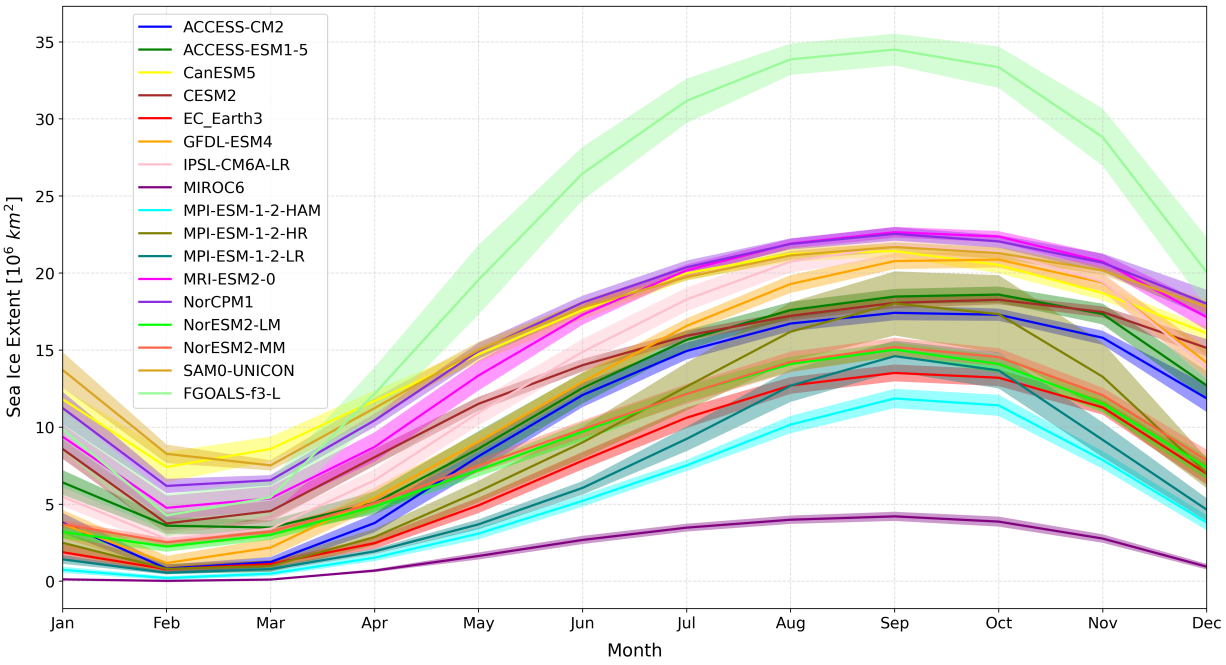

Figure 9: Pre-Earth observation era (1930-1939) sea ice extent seasonal cycle climatology for the 17 selected climate models. Colour-corresponding shaded areas represent the standard deviation over the decade for each respective climate model.

The results of the climatological sea ice extent seasonal cycle, in Figure 9 vary between individual climate models. The spread is wider in the austral winter than in the austral summer. There are some outlier models such as FGOALS-f3-L, showing a very intense climatological seasonal cycle while MIROC6 is showing a very small seasonal cycle. Most of the models are illustrating a narrow standard deviation over this decade, barring FGOALS-f3-L and MPI-ESM-1-2-HR.

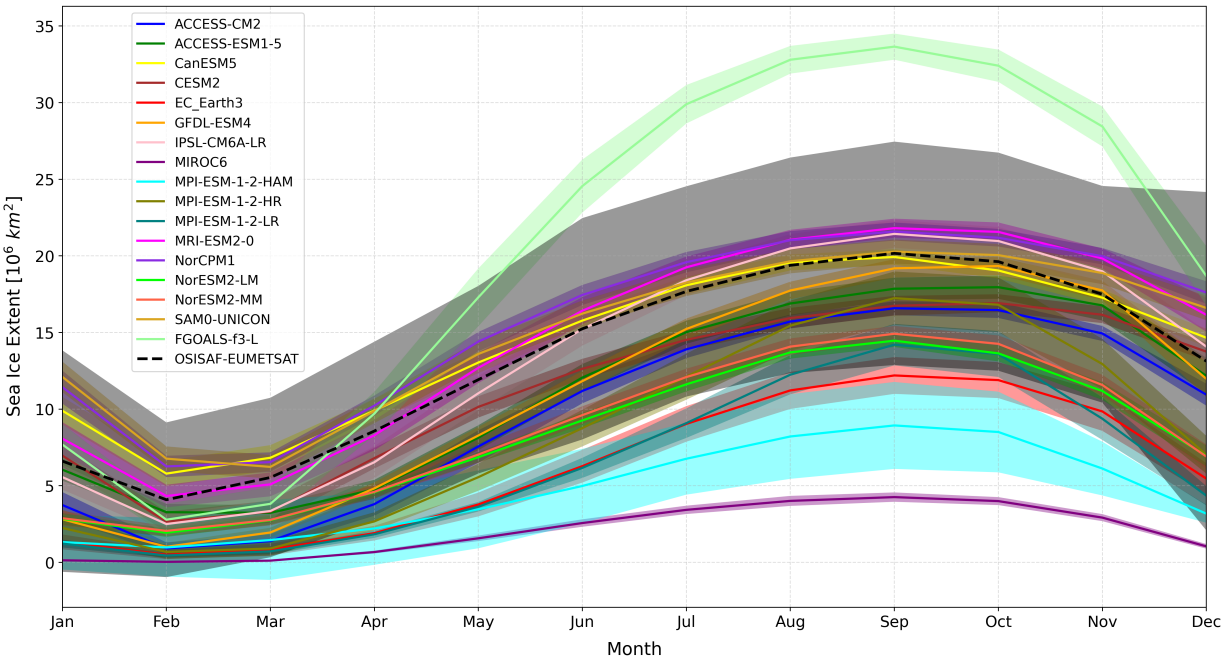

Figure 10: Earth observation era (1979-2014) sea ice extent seasonal cycle climatology per climate model and contemporary satellite observations from the ESA-CCI CDR (Section 2.1.3, dashed black line). Colour-corresponding shaded areas represent the standard deviation over the period for each respective climate model and for the satellite observations (in dark grey).

The results of the climatological sea ice extent seasonal cycle, in Figure 10 vary between individual climate models. The spread, much like in Figure 9, is much wider in the austral winter than in the austral summer. The majority of the models underestimate the climatological sea ice extent seasonal cycle, based on previous literature described in Section 2.2.2. There are a couple of outliers, particularly in their austral winter peak results, such as FGOALS-f3-L and MIROC6, a feature that was also observed earlier in the century (Figure 9). From this figure, the selected 1^{st}-rated climate models are CanESM5, CESM2, MRI-ESM1-5, NorCPM1 and SAM0-UNICON, based on the mean bias described in Section 2.2.2. These models are more likely to produce the most reliable sea ice edge results also during the pre-Earth observation era, compared to the other models that do not produce curves that have as close of a proximity to the satellite observations. The selected 2^{nd}-rated climate models are ACCESS-CM2, ACCESS-ESM1-5, GFDL-ESM4 and IPSL-CM6A-LR.

Most of the models indicate persistence of the climatological sea ice extent seasonal cycle features between the pre-Earth observation era and the Earth observation era. The models that show a general decrease of the mid-summer (January) extent are CanESM5, CESM2, FGOALS-f3-L, MRI-ESM2-0, NorCPM1 and SAM0-UNICON. Some others show a change in their standard deviations. For example, in models EC_Earth3, MPI-ESM-1-2-HAM and MPI-ESM-1-2-LR, the standard deviation increases from the pre-Earth observation reference period to the Earth observation era.

It is thus interesting to investigate the trends in the summer conditions, which is the period of the whale catch data. Figures 11 and 12 show the annual summer mean time series of sea ice extent for the

20^{th} century, with the extended summer definition being consistent with the study - November, December, January and February. For simplicity, the term "summer" will be used to refer to this extended summer period throughout the text. The analysis is presented separately for period 1900-1950 and period 1951-2014 for the two categories of climate models, the 1^{st}-rated models, and the 2^{nd}-rated models. A multi-decadal standard deviation was calculated over each respective period, for each climate model. This was to account for climate models trend, which is more visible in the later years, as described in Section 1.2.2.

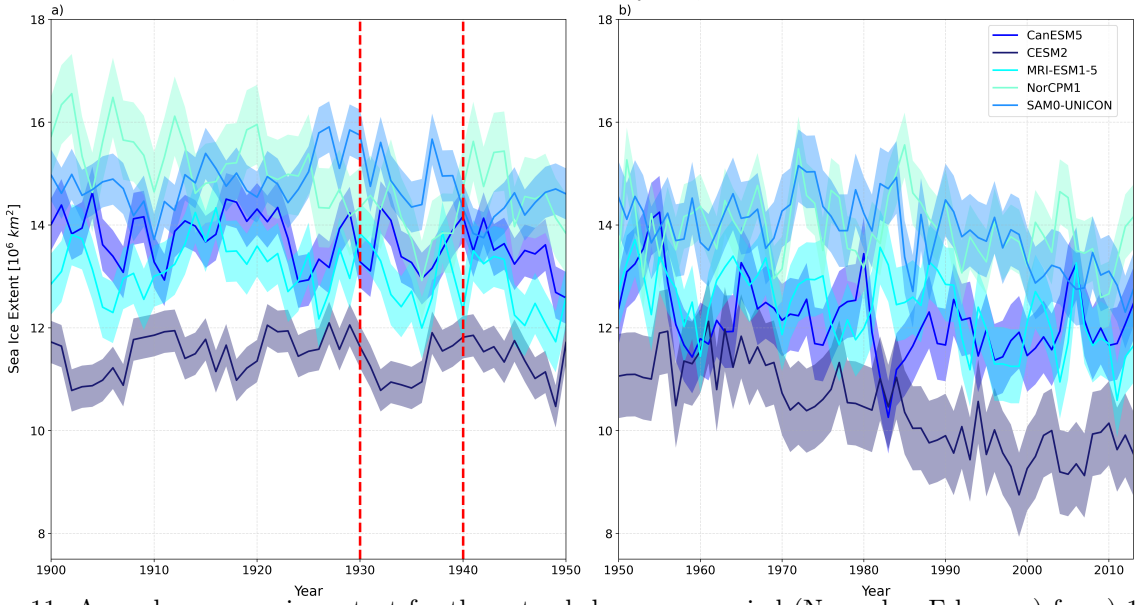

Figure 11: Annual mean sea ice extent for the extended summer period (November-February) for a) 1900–1950 and b) 1951-2014, produced by the 1^{st}-rated climate models available in the study. The red dashed line in panel a) represents the focus decade for the study, based on the whale catches. Colour-corresponding shaded areas represent the standard deviation, calculated over the period shown in each panel, for each climate model.

Although not the primary object, the sea ice extent annual summer mean time series, in Figure 11, shows the sea extent trend in the last century that was observed in the majority of CMIP5 models (for example, Hobbs et al., 2016).

This figure shows a number of important features. The first characteristic is the downward shift in annual summer mean sea ice extent after the '70s. Secondly, the standard deviation, mainly increases between periods ought to the presence of the trend. Table 5 below shows the numerical values of the standard deviations with respect to each period, illustrating the increase in standard deviation from period 1900-1950 to period 1951-2014. Finally, some models present a diminishing trend that is also visible in the period 1900-1950. One of the assumptions of this work is that the decade 1930-1939 is representative of ice conditions simulated by the climate models in the pre-Earth observation era. There is some inter-decadal difference in the annual summer mean for this period in some models, which have a standard deviation above 0.5 x 10^6 km ^{2} (Table 5). This value is about 5% of the long-term mean over the period . The decade 1930-1939 appears to be representative of the ice conditions during the pre-observation era for this category of models.

Table 5 presents the standard deviation for the 1^{st}-rated models, with respect to period 1900-1950 and period 1951-2014.

Table 5: Standard deviation of the sea ice extent annual summer mean time series for the 1^{st}-rated climate models for period 1900-1950 and period 1951-2014.

Climate Model	Standard Deviation [10^6 km^2]	
	1900-1950	1951-2014
CanESM5	0.505	0.705
CESM2	0.411	0.818
MRI-ESM1-5	0.595	0.719
NorCPM1	0.771	0.629
SAM0-UNICON	0.498	0.705

Table5 shows an increase in standard deviation of the annual summer mean of sea ice extent from the earlier period to the later period in the 20^{th} century.

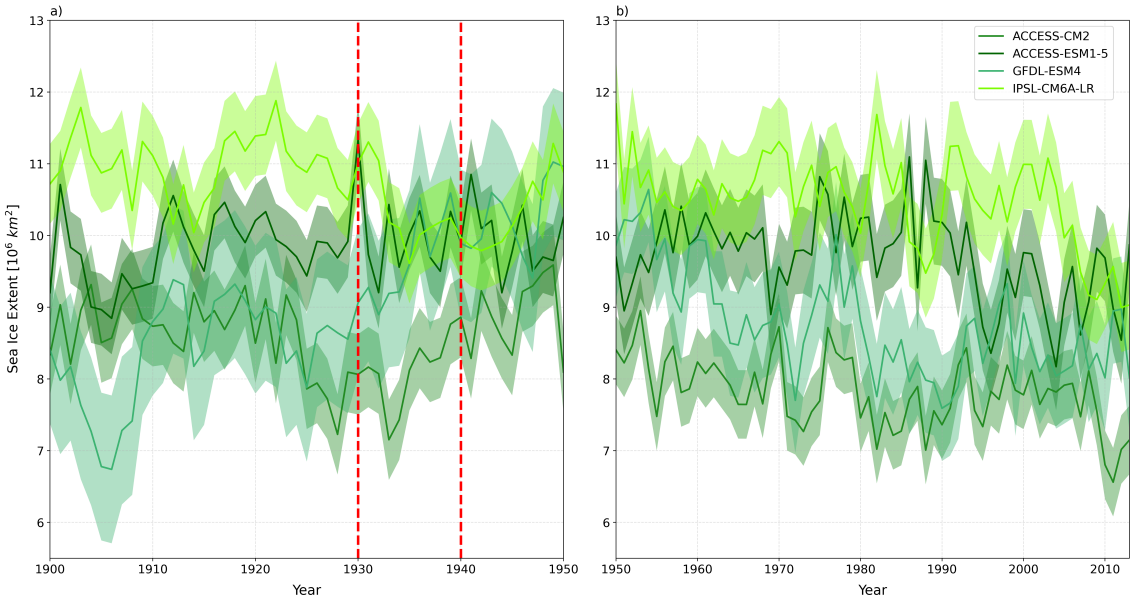

Figure 12: Annual mean sea ice extent for the extended summer period (November-February) for a) 1900–1950 and b) 1951-2014, produced by the 2^{nd}-rated climate models available in the study. The red dashed line in panel a) represents the focus decade for the study, based on the whale catches. Colour-corresponding shaded areas represent the standard deviation, calculated over the period shown in each panel, for each climate model.

Interestingly, the sea ice extent annual mean time series for the 2^{nd}-rated models in Figure 12 shows a smaller trend in the second half of the century. This observation contrasts the observation done for the 1^{st}-rated models in Figure 11. The models that depart more from the observed seasonal climatology of sea-ice extent seem to have a reduced declining trend during the more recent period.

Figure 12 shows a downward shift in the early 2000s. The standard deviations for each model between the two 50 years periods remains similar (Table 6). This is with the exception of model GFDL-ESM4 which has a larger increasing trend in the period 1900-1950, and a smaller decreasing sea-ice extent in 1951-2014. This model behaviour may thus indicate an adjustment from low sea-ice extent during pre-industrial conditions,

and then another adjustment when the tropospheric warming increases.

Table 6 presents the standard deviation for the 2^{nd}-rated models, with respect to each period.

Table 6: Standard deviation of the sea ice extent annual summer mean time series for the 2^{nd}-rated climate models for period 1900-1950 and period 1951-2014.

Climate Model	Standard Deviation [10^6 km^2]	
	1900-1950	1951-2014
ACCESS-CM2	0.560	0.477
ACCESS-ESM1-5	0.501	0.605
GFDL-ESM4	1.030	0.734
IPSL-CM6A-LR	0.557	0.621

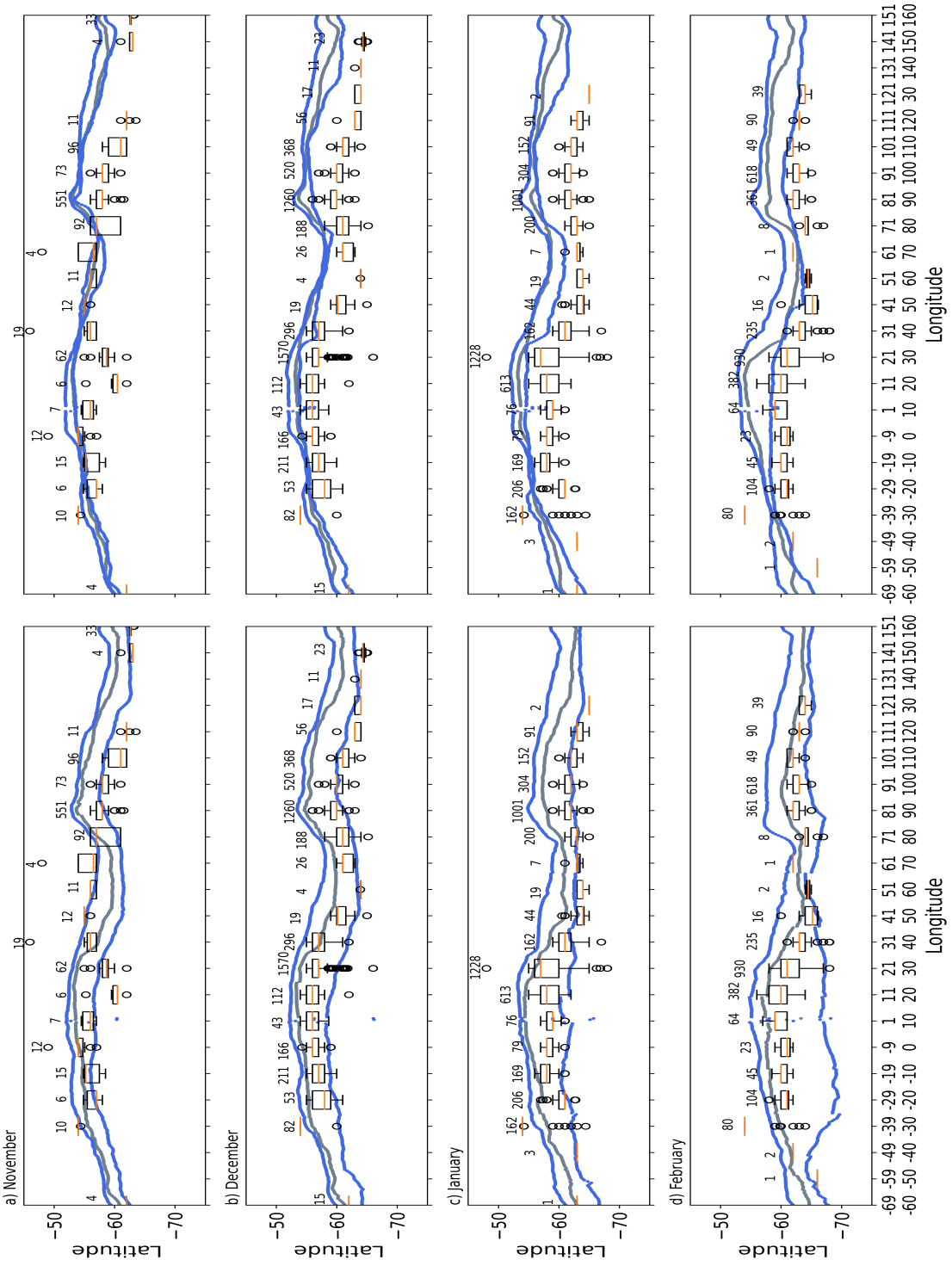

Figure 13: Multi-model distribution of the median sea ice edge location analysis from the pre-Earth observation reference period compared to the reconstructed ice edge distribution from humpback whale catches for a) November b) December c) January and d) February. When viewing the figure in landscape, the left column is the median location from all the 23 climate models. The right column shows only the 1^{st}-rated climate models. The 25^{th} and 75^{th} percentiles are indicated by the blue lines and the median is indicated by the grey line. The whale catch numbers, per longitudinal bin, are annotated above each box plot.

3.3 Comparison of Sea Ice Edge Reconstructions

Figure 13 presents the sea ice edge location analysis for the pre-Earth observation era.

In both columns, the spread in the ensemble median of the simulated sea ice edge locations increases with the progression of the austral summer (Table 7). This indicates that the timing of the melting initiation is different in the individual models. Both ensemble distributions also show the simulated sea ice edge median location to be positioned north of the reconstructed whale catch distributions, also considering the inter-quantile ranges of the individual latitudinal bins. Additionally, the modelled edge location patttern seems to follow the latitudinal pattern of the whale catch distribution quite well, especially in January when the extent is more reduced in the Indian sector between 30 and 80°E.

The distribution of the decadal ensemble median from the 1^{st}-rated models is narrower (right column) than the 23-model ensemble distribution (left column). This suggests stronger agreement between the models that are classified to be the best ones when compared against contemporary satellite data.

The all-model ensemble shows this feature only for the 75^{th} percentile and the median, which remain close to each other throughout the austral summer season. The larger spread of the 25^{th} percentile could be representative of a few models that simulate very low sea ice extent and hence present a more southward location of the edge. Underestimating models would contribute to the higher spread in the 23-model distribution.

Table 7: Sea ice edge inter-quartile range for both multi-model distributions in Figure 13, for each month in the study.

Month	Mean IQR (km)	
	All 23 models	1^{st}-rated models
November	396	146
December	557	219
January	720	275
February	864	431

Table 7 presents the inter-quartile range of the sea ice edge location computed for the 23-model distribution and for the 1^{st} -rated models, for each selected month of the study. There is an increase in sea ice edge location distribution spread with the progression of the austral summer. This is more evident for the 23-model distribution and between January and February in the 1^{st} -rated models. Table 7 also shows that there is a decrease in sea ice edge ensemble distribution spread from the 23-model distribution to the 1^{st} -rated models, for all selected months of the study.

To better quantify if the pattern of the simulated ice edge follows the one derived from whale catches, Figure 14 shows a latitudinal linear correlation plot between the median location from climate models and the whale catches. The resulting statistical test shown in Table 8 was carried out using the Spearman's correlation test due to the non-Gaussian distribution of the data. The coefficient of determination was also used to measure the spread of the data around the 1:1 line.

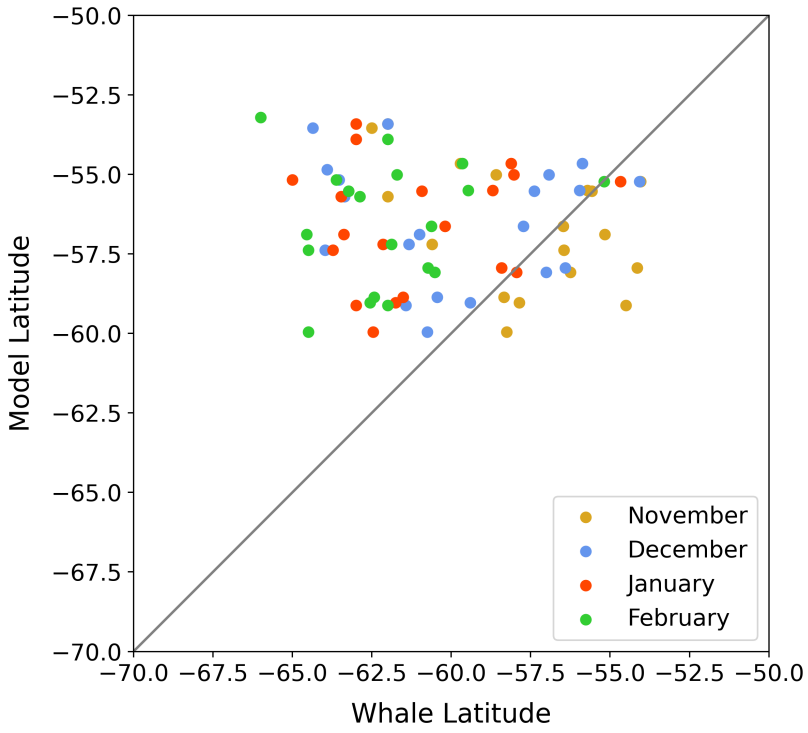

Figure 14: Pre-Earth observation correlation between the sea ice edge location result of the 1^{st} -rated model distribution and the whale catch distribution, for each month in the study. The correlation is plotted against a one-to-one reference line.

The spread of the data around the 1:1 line changes with the month of analysis, with the strongest correlation visibly found in November. As the summer progresses, the correlation weakens; with the weakest correlation being in February. In this month, the whale-derived edge location median clusters around 62.5ºS within a range of 5 degrees latitude, while the model spread is larger and centered around 57.5ºS. The compact structure of the clusters suggests that there is some agreement between both variables, however carrying latitudinal bias. The climate models also show a latitudinal constraint within the range of 52.5ºS and 60ºS, for all months. The latitudinal rigidity in the climate model results throughout each month of the study may point to a constraint imposed through tuning against the contemporary satellite data or to the lack of physical processes in the sea ice dynamics.

Table 8: Pre-Earth observation coefficient of determination and Spearman's test results for the correlation between the sea ice edge location result of the 1^{st} -rated modeldistribution and the whale catch distribution for each month of the study.

Month	R^2	r	p-value
November	0.185	-0.361	0.141
December	0.003	-0.075	0.753
January	0.013	0.056	0.819
February	0.011	0.116	0.637

The coefficient of determination shows how much the 1^{st} -rated models can explain the whale catch

distribution variance. Table 8 shows that November has the highest explained variance, with a value of 0.185. This value is however very small, indicating that only a portion of the simulated edge follows the reconstructed sea ice features. The apparent visual agreement in November is therefore not corroborated by a more objective measure of relationship.

The table also shows the Spearman's test results for the correlation between the sea ice edge location result of the 1^{st} -rated models and the whale catch distribution, for each selected month in the study and the related p-value.The correlation values, r, are all close to 0, signaling very weak correlation. The negative r values in the months of November and December indicate opposing latitudinal patterns between the 1^{st} -rated models and the location of whale catches. This opposition can be actually seen in Figure 13 between 11ºE - 90ºE for November and 49ºW - 30ºW for December. All p-values are above 0.05, indicating no significance of any correlation measure.

4 Summary and future works

Interdisciplinary scientific research is important because it offers a more holistic understanding of the broad and far reaching impacts of the changing natural environment, giving us the opportunity for better-informed decision making. Anthropogenic pressures on the natural environment, such as the industrial era that has resulted in a 1^{o}C global temperature rise since the pre-industrial era, can be linked to some of the observed changes in our oceans and cryosphere. These changes in turn strongly influence how our climate is changing. Changes in the ocean and cryosphere also impact the natural marine ecosystems, which through their biodiversity, provide us with important ecosystem services.

The study of humpback whales offers a unique window of opportunity for interdisciplinary scientific research due to their ecological behaviour and endurance through anthropogenic pressures. This study used the interdisciplinary approach to explore the intersection between their ecology and oceanographic features to lend to the assessment of climate projections.

The study aimed to assess 20^{th} century climate model sea ice edge results in the Southern Ocean, against humpback whale catch distributions. The study also aimed to assess climate model sea ice extent results against contemporary observations as well as compare results between individual models. By carrying out these analyses, climate model results can suggest where climate models are doing well and where they need evaluating. The continuous assessment of climate models is important in increasing their reliability in climate projections. Due to the lack of observational data in this remote region during the early 20^{th} century, climate model verification against observations is limited for this period.. There is no work-around for this challenge other than to increase assessment against observational data, where possible. Therefore, although the whale catch data carry inherent biases, they offer strongly-lending Antarctic oceanographic data for the early 20^{th} century which can be used to to fill data gaps. This study indicates that climate models are overestimating the sea ice edge results in the Southern Ocean based on the real data collected from whaling logs. These are certainly useful findings in that we can do further investigations to understand how climate models are simulating sea ice edge results in the highly complex Southern Ocean. Furthermore, these findings present the opportunity to possibly improve sea ice edge simulations in the Southern.

The humpback whale catch effort, as per IWC data, mostly covered the Atlantic and the Indian sector of the Southern Ocean. For this reason, the study focused on these two sectors for the analyses. Decade 1930-1939 showed the highest catch numbers consistently throughout the months of the study. Sea ice extent analyses were carried out in this study because of the close relationship sea ice extent has with sea ice edge. The availability and use of contemporary satellite observations allowed for sea ice extent analyses in both the pre-Earth observation and the observation era. Observational data only began to increase in frequency and consistency in the mid-20^{th} century. Prior to these developments, the understanding of the changing climate in the Southern Ocean over earlier periods is limited. Sea ice extent was used as both an assessment and comparison indicator. The climatological sea ice extent seasonal cycle results for the pre-Earth observation era varied largely between models, especially in the winter, with the majority of the climate models underestimating the climatological seasonal cycle of sea ice extent, based on previous literature. There were also some outlier models presented in this analysis, such as FGOALS-f3-L and MIROC6.

The climatological sea ice extent seasonal cycle results for the observation era also varied largely between models , with the majority of the models not exceeding a 20 million km^2 winter maxima. The models do not seem to capture the seasonal cycle very well, contrary to Zunz et al. (2013) findings. This suggests

that there may be little difference between CMIP5 and CMIP6 climatological sea ice extent seasonal cycle projections.

By assessing the climatological sea ice extent seasonal cycle results for the observation era against the contemporary observations, 1^{st}-rated and 2^{nd}-rated models were chosen, based on their proximity to the satellite observations. Using these two classes of models, the persistence of the simulated sea-ice features between the two observation eras was compared, using the annual summer mean sea ice extent as the reference variable. The annual summer mean sea ice extent time series from both model classes illustrated that in a time when data is lacking, the majority of the highest-rated models show reduced variability, apart from a few notable exceptions. Therefore the decision to make decade 1930–1939 a representative of a pre-Earth observation era is acceptable.

The second assessment indicator variable used in the study was the latitudinal location of sea ice edge. Knowing that humpback whales were caught at a proximity to the ice edge, this variable was used as a benchmark against the simulated sea ice edge. The overall pattern of the ensemble median of the modelled ice edge location apparently follows the latitudinal pattern of the whale catch locations, which are assumed in this study to mark the topography of the sea ice edge. A more accurate analysis based on the linear correlation however indicated that the coefficient of determination is different from zero only in November, and even in this case, the correlation is negative. According to Roach et al. (2020) CMIP6 models improved their geographical distribution of SIC from CMIP5 when compared against satellite data. The comparison with historical proxy observations instead reveal a different pattern. In particular, the early 20th century ensemble median of the simulated sea ice edge is substantially northward of the whale catch distribution. This was more clearly illustrated in the 1^{st} -rated models results of the sea ice edge. The much narrower mean sea ice edge distribution inter-quartile range in the 1^{st} -rated models than in the full 23-model distribution, means that the 1^{st} -rated models were in strong agreement of their results, and they all overestimated the northward location of the ice edge against the proxy data.The correlation plot of the 1^{st} -rated models illustrated latitudinal rigidity in climate model mean sea ice edge location, producing results that were contained within a latitudinal range of 52.5 ^{o}S - 60 ^{o}S. This is the same latitudinal range of the warmer waters found around the dynamic Antarctic Circumpolar Current (Nghiem et al., 2016). The plot also illustrated a seasonal variation in results, with November showing the strongest correlation. This may possibly be due to the diffuse nature of sea ice in the summer months, especially late summer months, creating disparity in sea ice definition (Eayrs et al., 2019).

The whale catch distribution showed very little catch logs in the Pacific sector of the Southern Ocean, see Figure 7. The Pacific region was, historically, a difficult area to whale due to the lack of land masses to provide harbouring or even to be used as processing stations. With that being said, humpback whales could have been present in the Pacific sector but due to the lack of whaling in the area, and the lack of observations in the area in the last century, the humpback whale distribution is largely unknown in this area for the last century. Therefore, another type of dataset will need to be used to carry out a similar assessment in this area of the Southern Ocean.

The varying results of the climatological sea ice extent seasonal cycle, for the pre-Earth observation era, between models could be due to the different constraints used by each model. Understanding how each model applies constraints is an important exercise to accurately interpret its outputs. For the observation

era, determining the relationship between SIC and sea surface temperature in models may give indication as to why models underestimate the summer sea ice minima (Roach et al., 2020), for example in model MIROC6.

How models results may differ from the start of the century to when observational data started being available is unclear - it could be that the models capture a trend over the last century or that there was a parameterization shift in the sea ice extent boundary conditions. For example, reasons for GFDL-ESM4 producing a very low summer mean sea ice extent in the first decade of the 21^{st} century are yet to be analysed. A quantitative analysis for this visual analysis in the persistence of climate model output between the two observation eras will improve the confidence of the finding. The increase in standard deviation in some of the models, from the pre-Earth observation era to the observation era may be due to an increase in constraints being used in some of the models. Further work in this regard would be a useful supplement in understanding the sea ice extent projections by each model.

While the physical laws employed by climate models to determine mean sea ice edge capture certain features, it is unclear whether the parameterization of individual climate models capture a calculated a shift in the initial boundary conditions or the change in sea ice behaviour with time.

The implication of overestimating sea ice edge in the Southern Ocean is that climate projections will be skewed in the Southern Hemisphere. As we know that the Southern Ocean makes a great contribution to climate regulation in the Southern Hemisphere, it is important to get the most accurate initialization in the Southern Ocean to yield the most reliable results. Nghiem et al. (2016) describes that warmer waters play a significant role in constraining the extent of sea ice and that these waters and their associated polar currents are subject to topographic steering. Therefore, understanding the climate model sea ice edge results may also need the consideration of other indicators such as sea surface temperature and bathymetry.

There are more recent data of whale sightings that have been collected over various Southern Ocean research cruises, such as the Southern Ocean Whale and Ecosystem Research Programme (SOWER)[9] and the Southern Ocean Research Partnership (IWC-SORP)[10]. These data provide an opportunity to carry out the same assessment as this study, where climate model mean sea ice edge results for the late 20^{th} century can be assessed against humpback whale sightings. This data will also likely carry less biases (See Section 2.1.1) than the commercial whaler's logs. Additionally, whale sightings in the Pacific are likely to be available, giving opportunity to carry out the assessments in the entire Southern Ocean.

The findings of this study certainly show that climate models are overestimating the sea ice edge in the Southern Ocean based on the real data collected from whaling logs. This raises the need for further analyses of sea ice climate model results in this region. The Southern Ocean and the Antarctic cryosphere play a vital role in the changing of our climate. We therefore need to continue to assess climate model results in the region so as to improve on our understanding and projections on the dynamics that exist within it.

[9]https://iwc.int/sower
[10]https://iwc.int/sorp

5 Appendix

Appendix A Figure 15 presents a graphical display of annual whale catches for each selected month of the study.

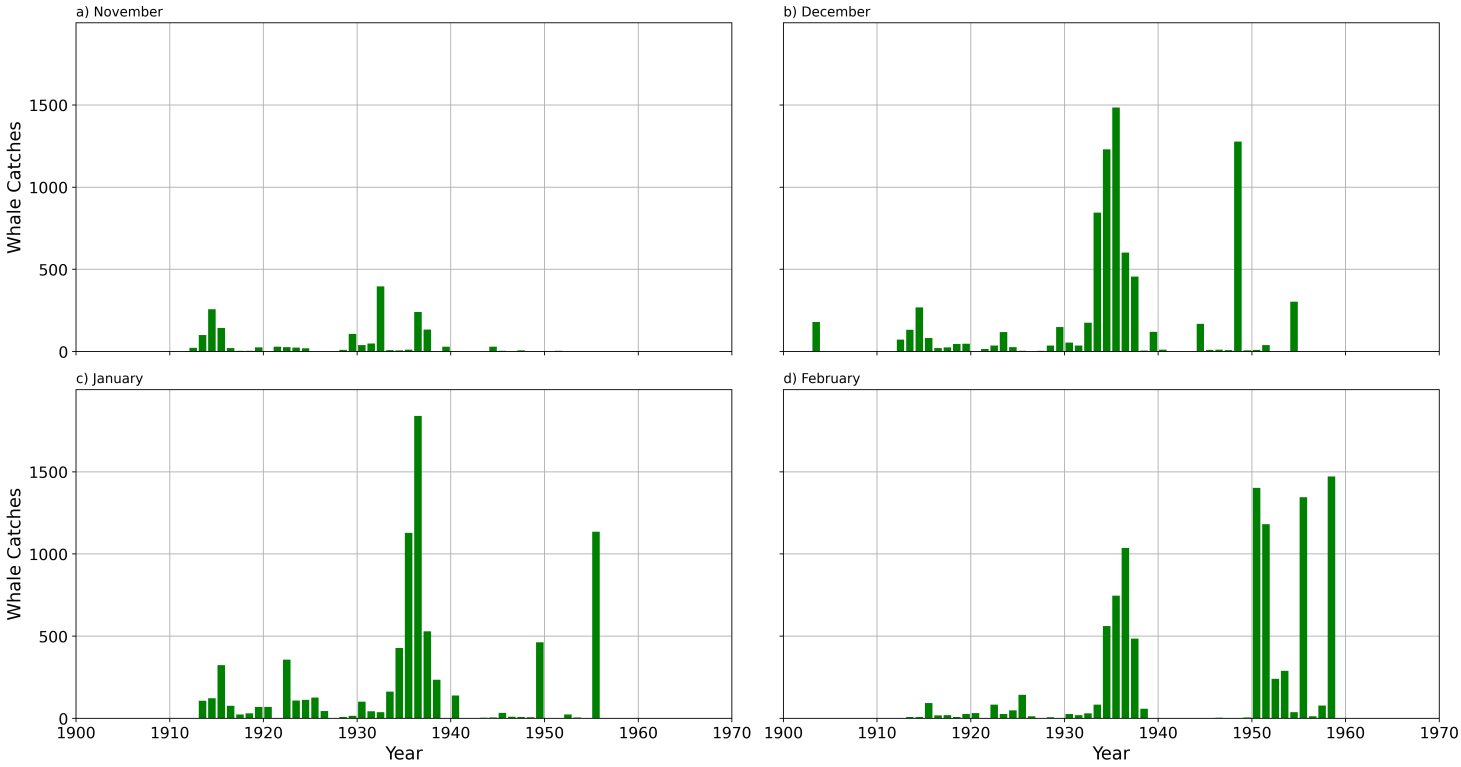

Figure 15: Annual humpback whale catches in the last century for each month of the study, a) November b) December c) January d) February, from the IWC.

Appendix B Figures 15 - 31 present a monthly time series, for the previous century, of total Antarctic sea ice extent measurements for each climate model.

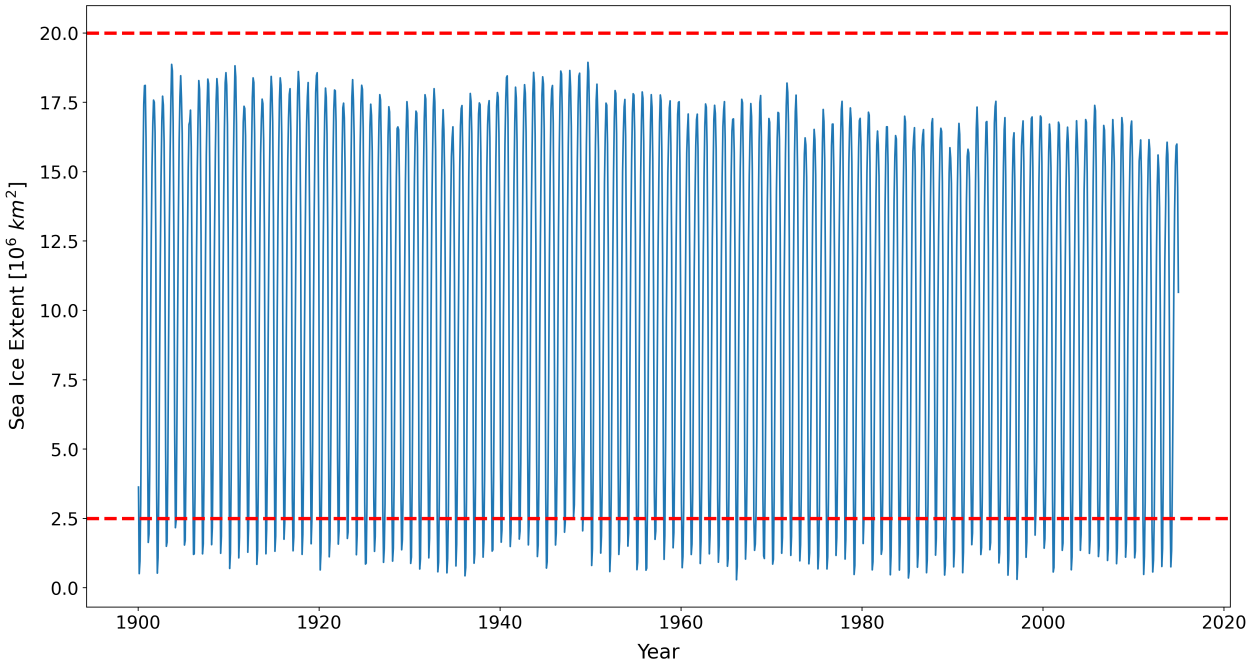

Figure 16: Annual sea ice extent seasonal cycle time series for the previous century, produced by climate model ACCESS-CM2. Red lines demarcate sea ice extent seasonal minimum and maximum based on previous literature (See Section 2.2.2).

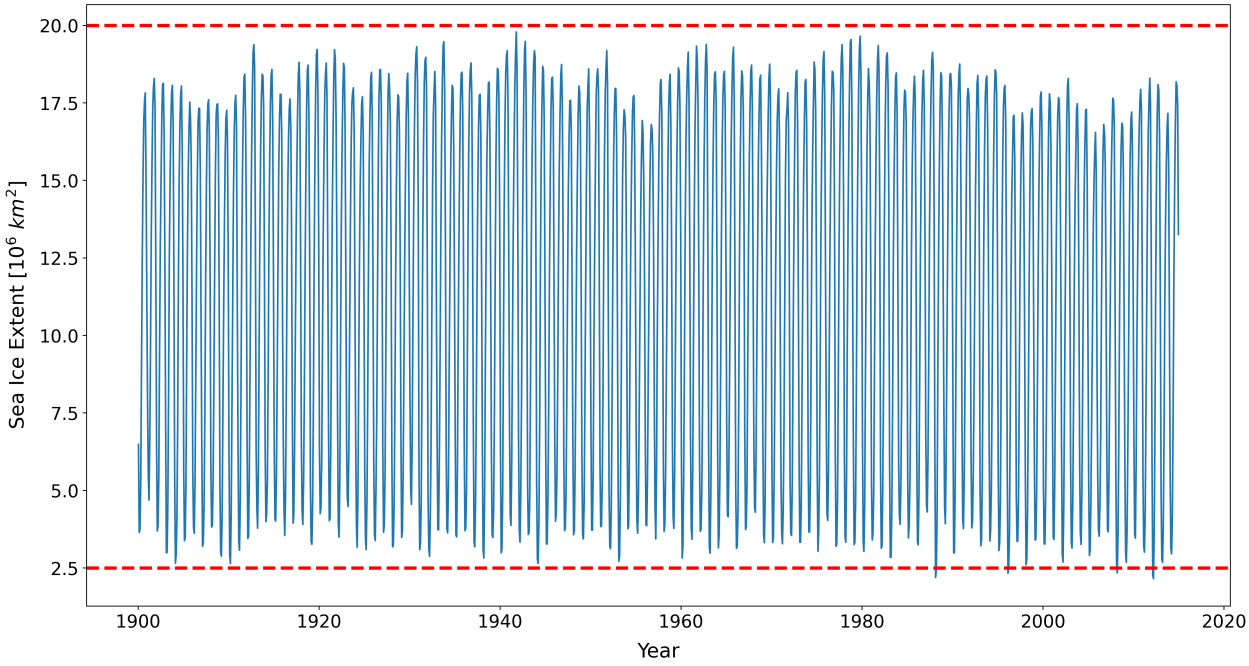

Figure 17: Annual sea ice extent seasonal cycle time series for the previous century, produced by climate model ACCESS-ESM1-5. Red lines demarcate sea ice extent seasonal minimum and maximum based on previous literature (See Section 2.2.2).

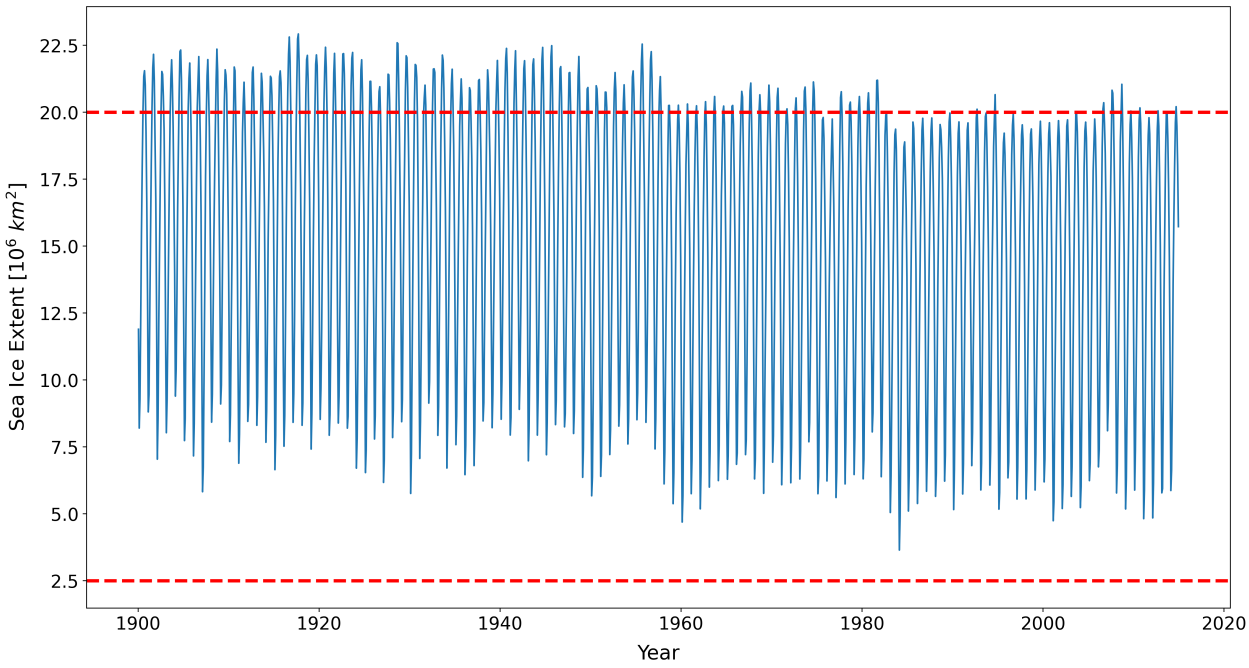

Figure 18: Annual sea ice extent seasonal cycle time series for the previous century, produced by climate model CanESM5. Red lines demarcate sea ice extent seasonal minimum and maximum based on previous literature (See Section 2.2.2).

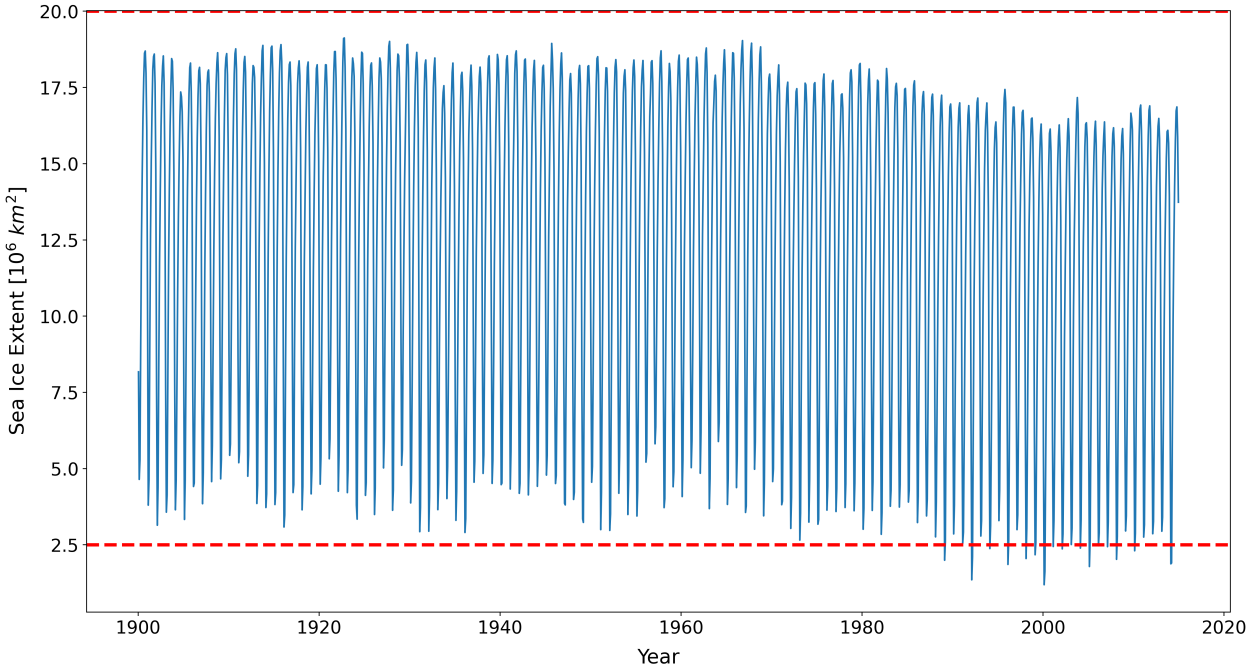

Figure 19: Annual sea ice extent seasonal cycle time series for the previous century, produced by climate model CESM2. Red lines demarcate sea ice extent seasonal minimum and maximum based on previous literature (See Section 2.2.2).

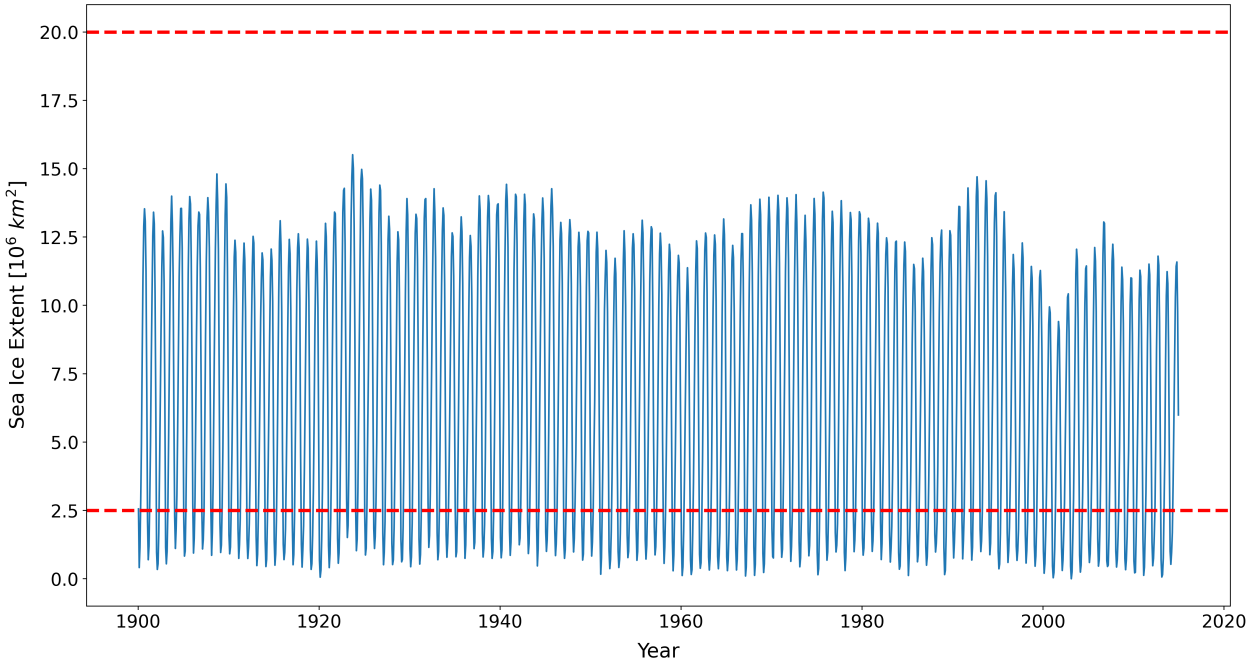

Figure 20: Annual sea ice extent seasonal cycle time series for the previous century, produced by climate model EC_Earth3. Red lines demarcate sea ice extent seasonal minimum and maximum based on previous literature (See Section 2.2.2).

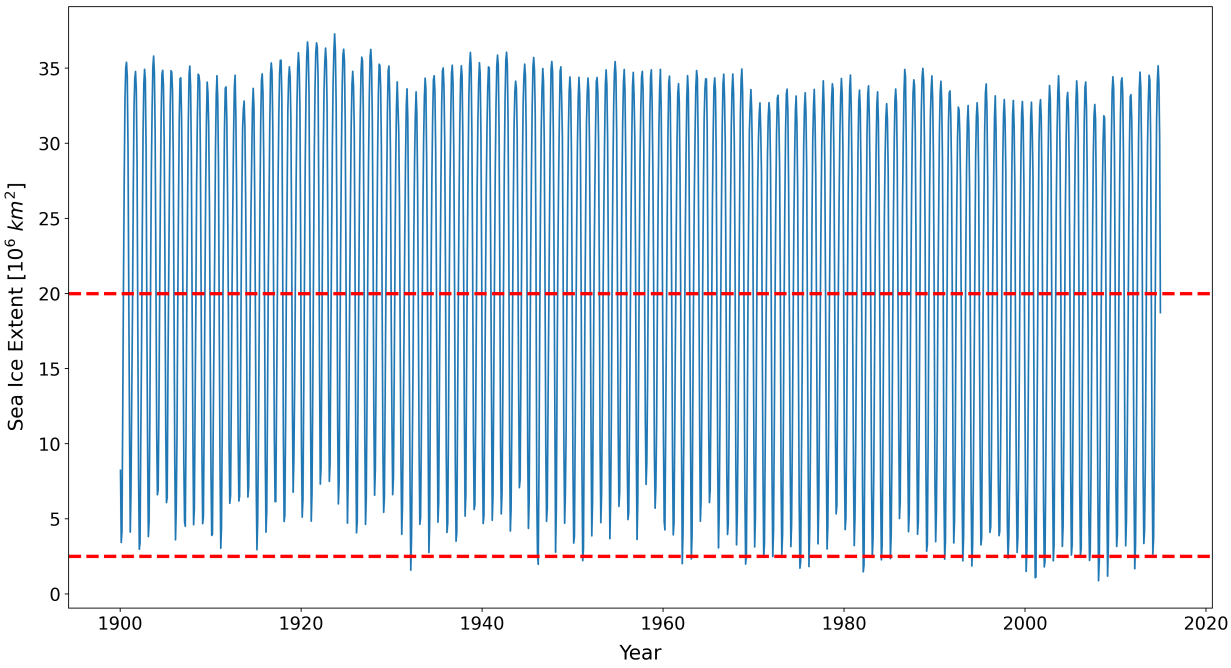

Figure 21: Annual sea ice extent seasonal cycle time series for the previous century, produced by climate model FGOALS-f3-L. Red lines demarcate sea ice extent seasonal minimum and maximum based on previous literature (See Section 2.2.2).

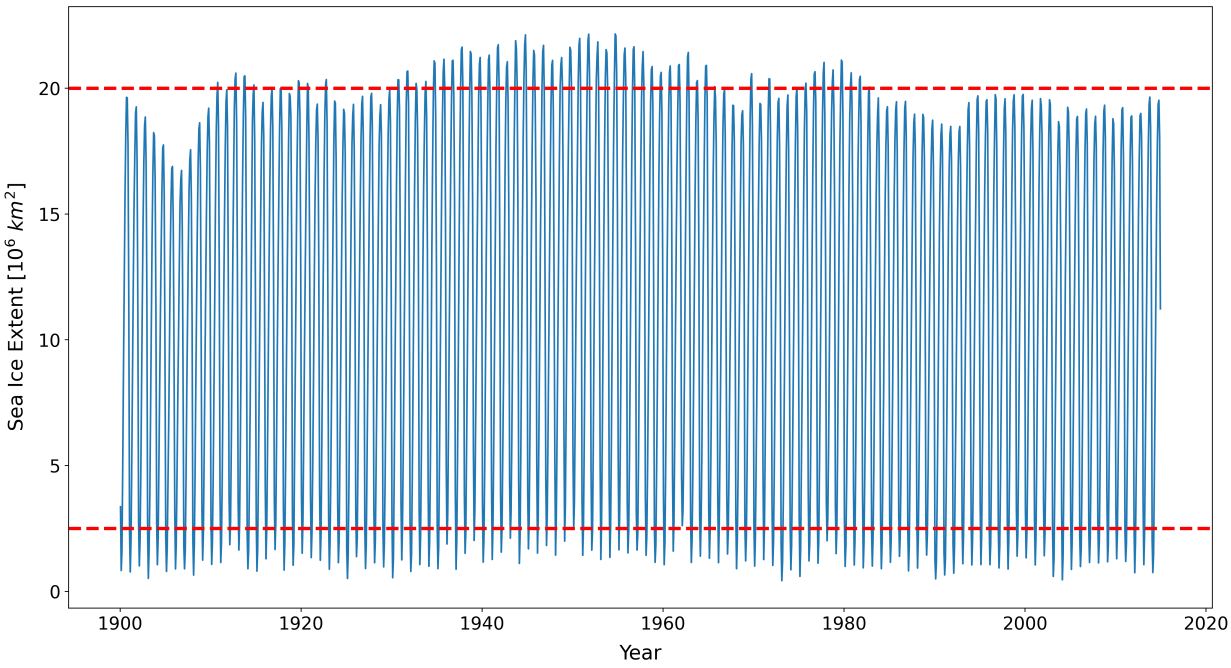

Figure 22: Annual sea ice extent seasonal cycle time series for the previous century, produced by climate model GFDL-ESM4. Red lines demarcate sea ice extent seasonal minimum and maximum based on previous literature (See Section 2.2.2).

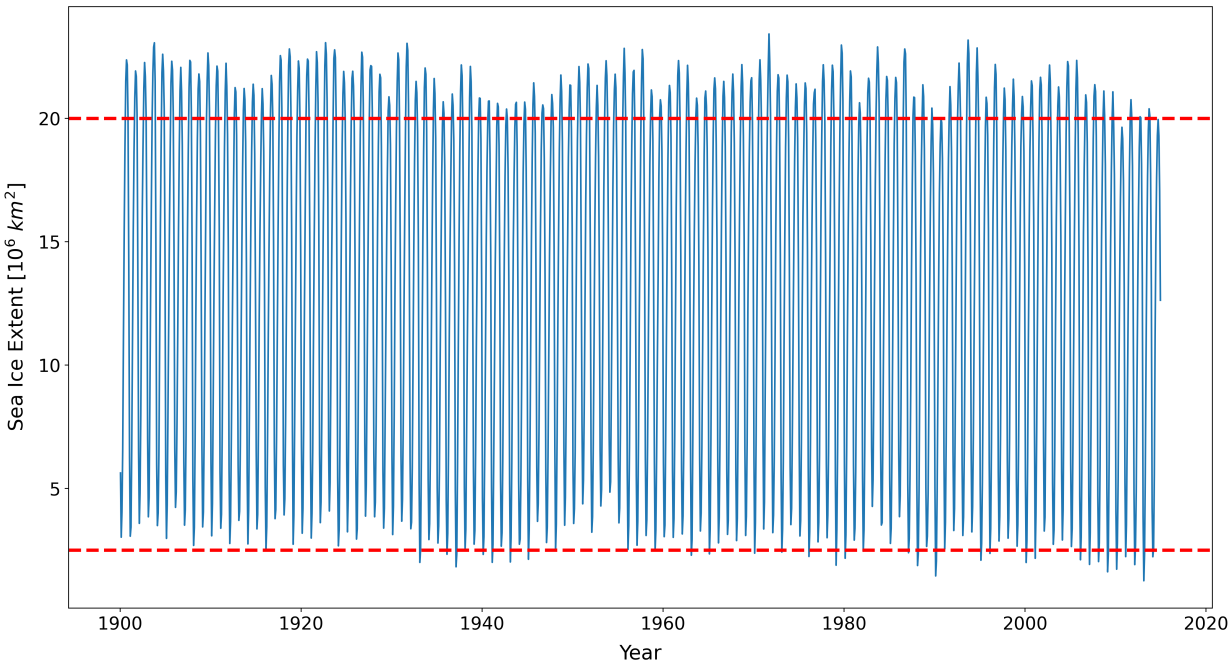

Figure 23: Annual sea ice extent seasonal cycle time series for the previous century, produced by climate model IPSL-CM6A-LR. Red lines demarcate sea ice extent seasonal minimum and maximum based on previous literature (See Section 2.2.2).

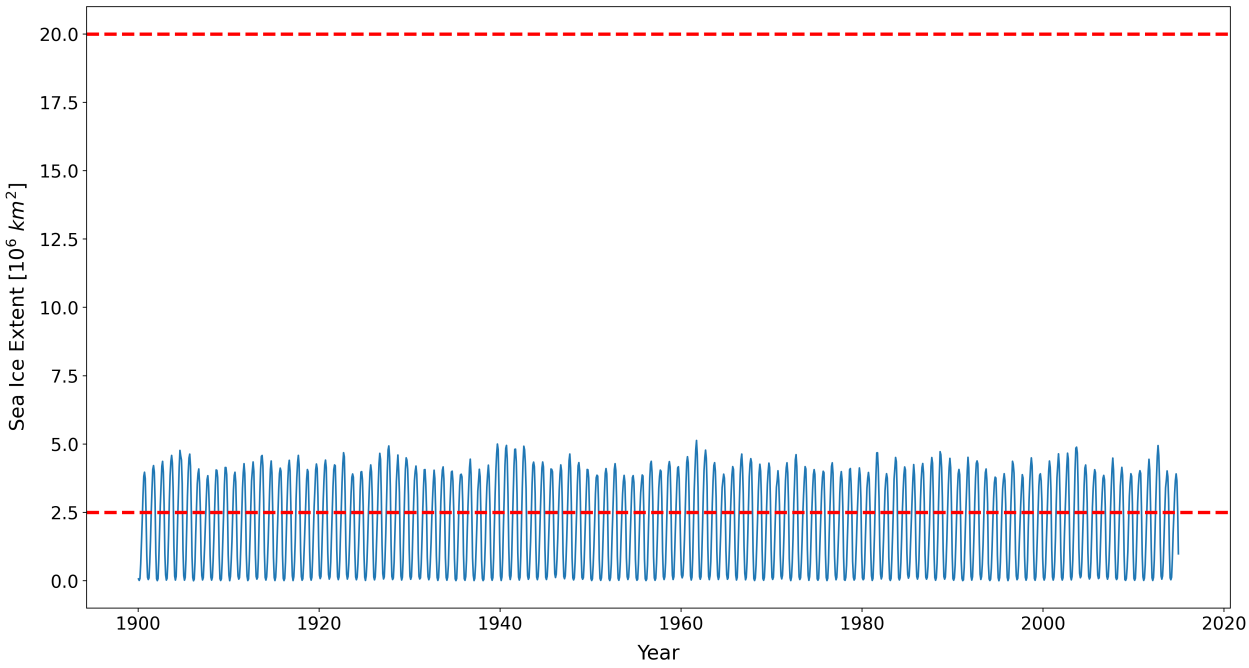

Figure 24: Annual sea ice extent seasonal cycle time series for the previous century, produced by climate model MIROC6. Red lines demarcate sea ice extent seasonal minimum and maximum based on previous literature (See Section 2.2.2).

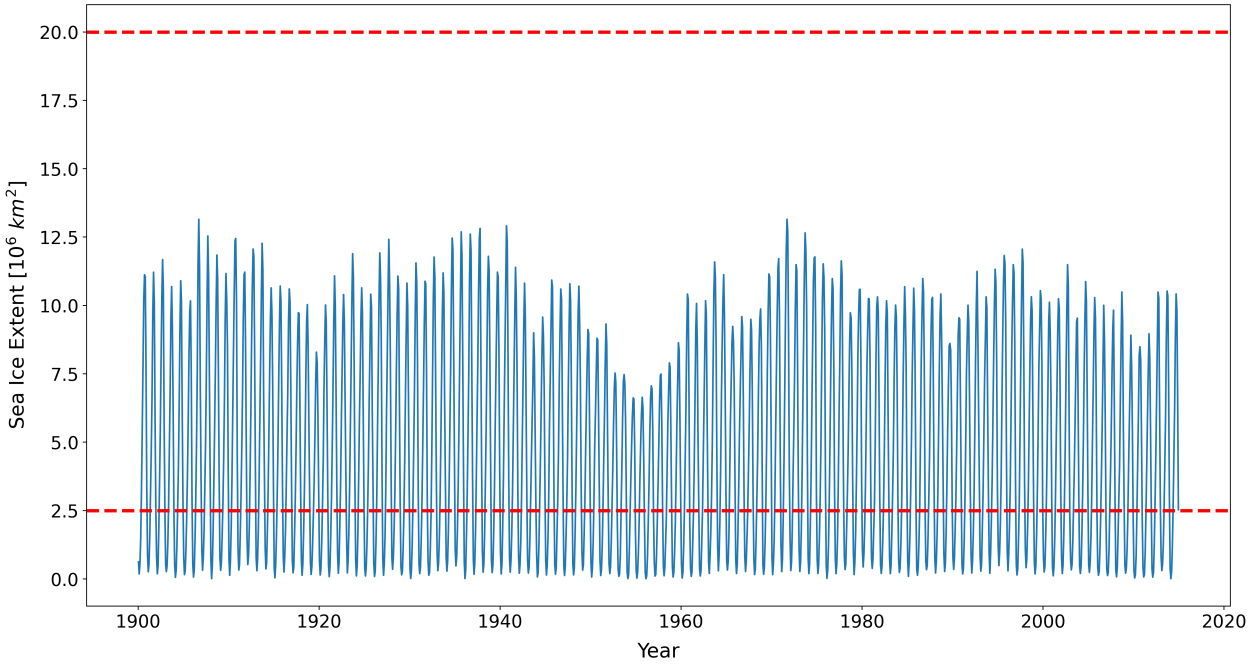

Figure 25: Annual sea ice extent seasonal cycle time series for the previous century, produced by climate model MPI-ESM-1-2-HAM. Red lines demarcate sea ice extent seasonal minimum and maximum based on previous literature (See Section 2.2.2).

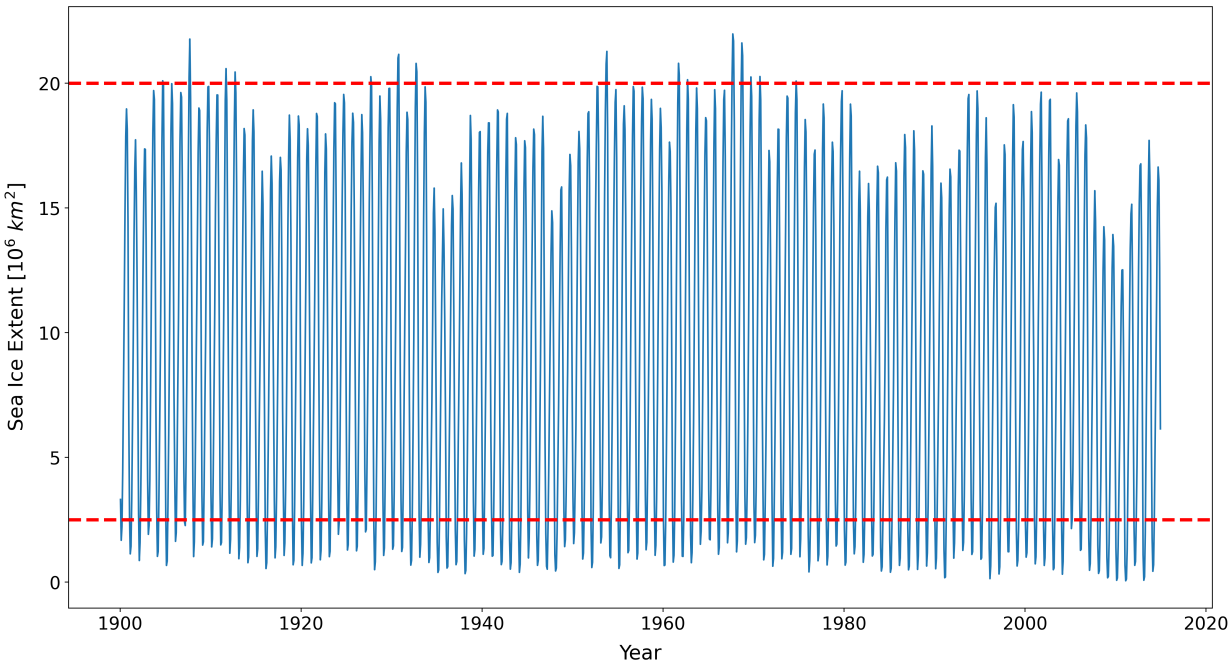

Figure 26: Annual sea ice extent seasonal cycle for the previous century, produced by climate model MPI-ESM-1-2-HR. Red lines demarcate sea ice extent seasonal minimum and maximum based on previous literature (See Section 2.2.2).

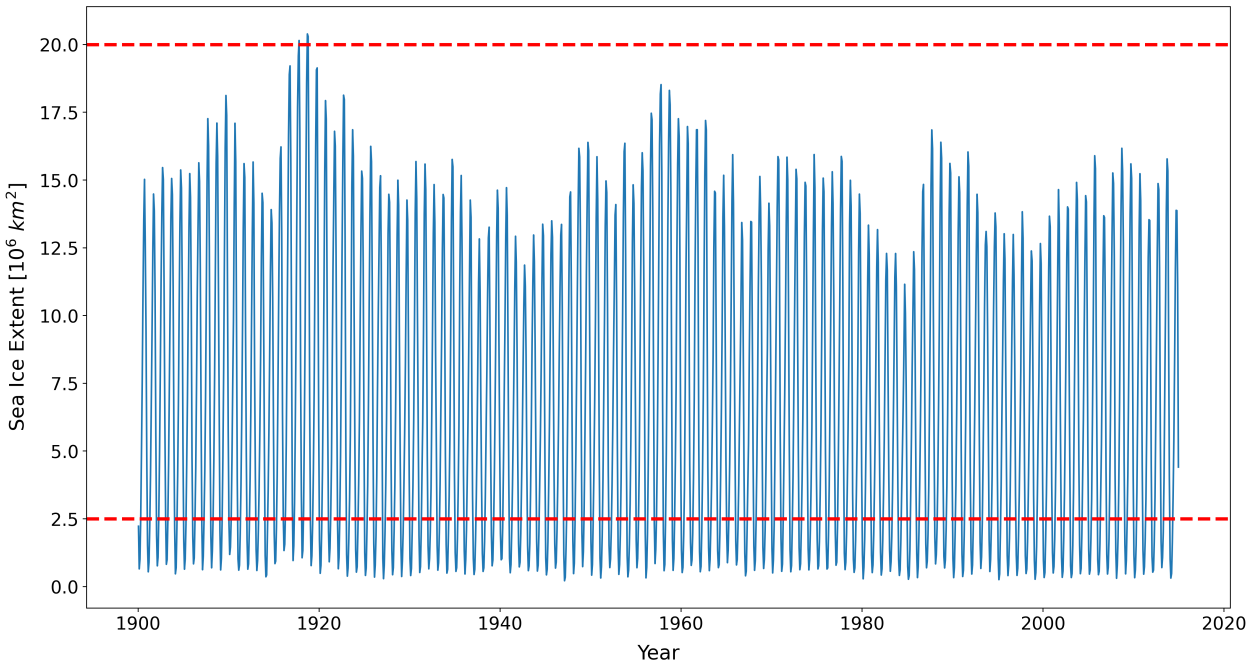

Figure 27: Annual sea ice extent seasonal cycle for the previous century, produced by climate model MPI-ESM-1-2-LR. Red lines demarcate sea ice extent seasonal minimum and maximum based on previous literature (See Section 2.2.2).

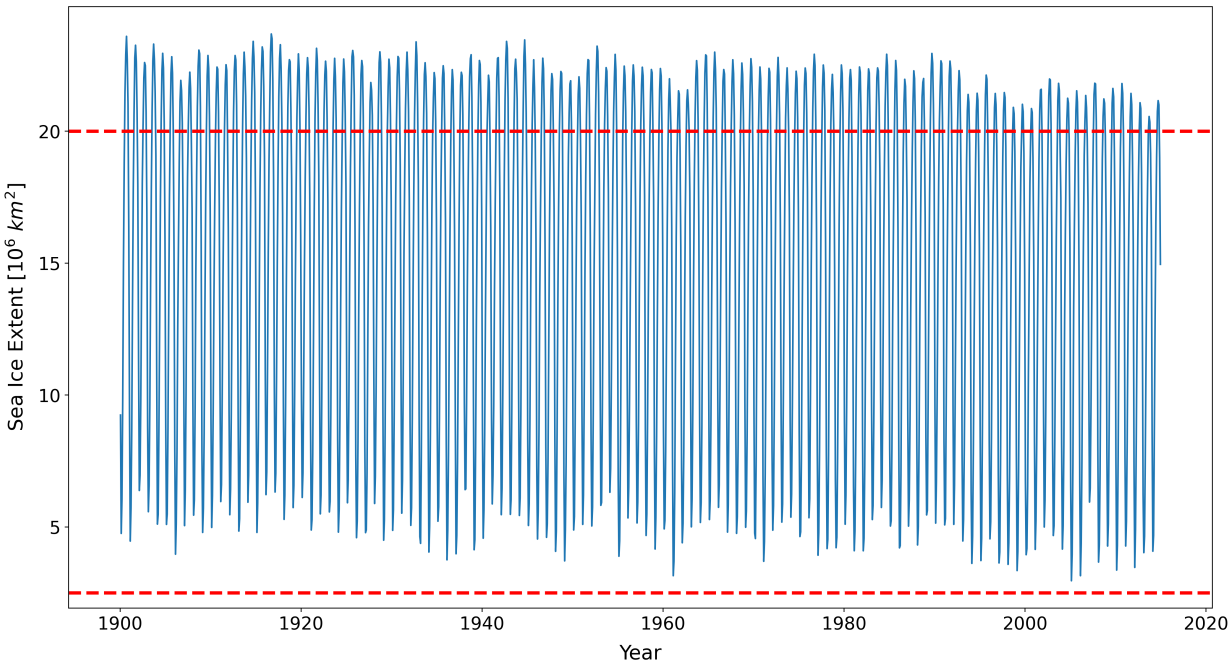

Figure 28: Annual sea ice extent seasonal cycle time series for the previous century, produced by climate model MRI-ESM2-0. Red lines demarcate sea ice extent seasonal minimum and maximum based on previous literature (See Section 2.2.2).

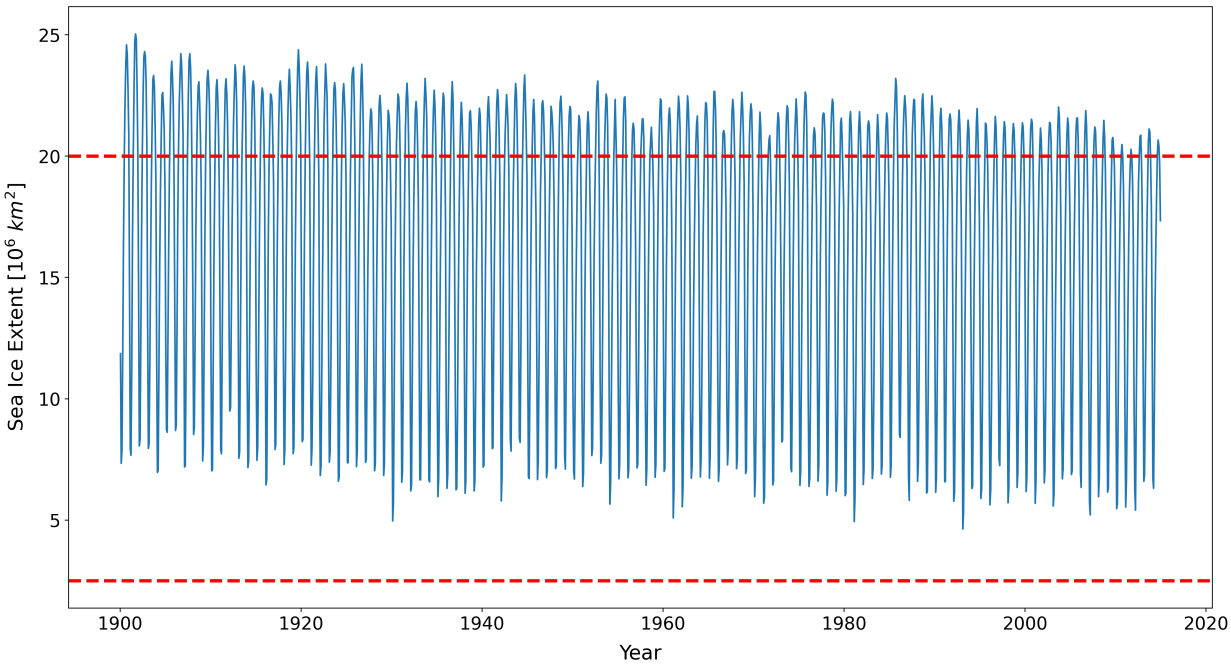

Figure 29: Annual sea ice extent seasonal cycle time series for the previous century, produced by climate model NorCPM1. Red lines demarcate sea ice extent seasonal minimum and maximum based on previous literature (See Section 2.2.2).

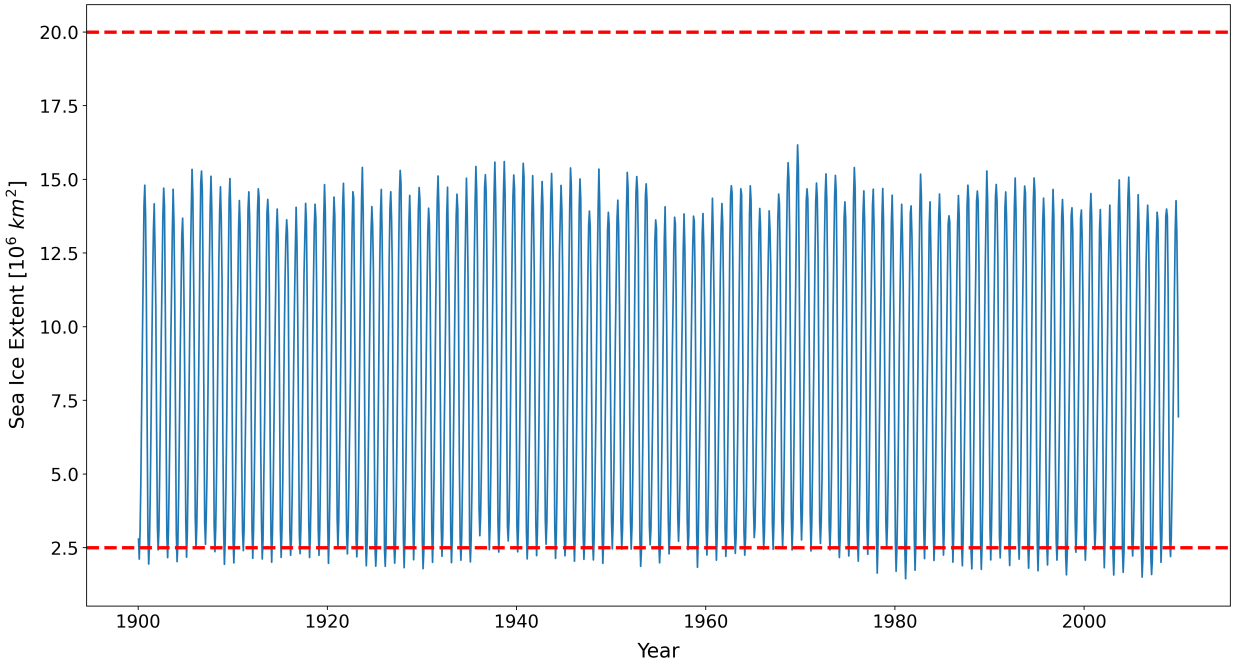

Figure 30: Annual sea ice extent seasonal cycle time series for the previous century, produced by climate model NorESM2-LM. Red lines demarcate sea ice extent seasonal minimum and maximum based on previous literature (See Section 2.2.2).

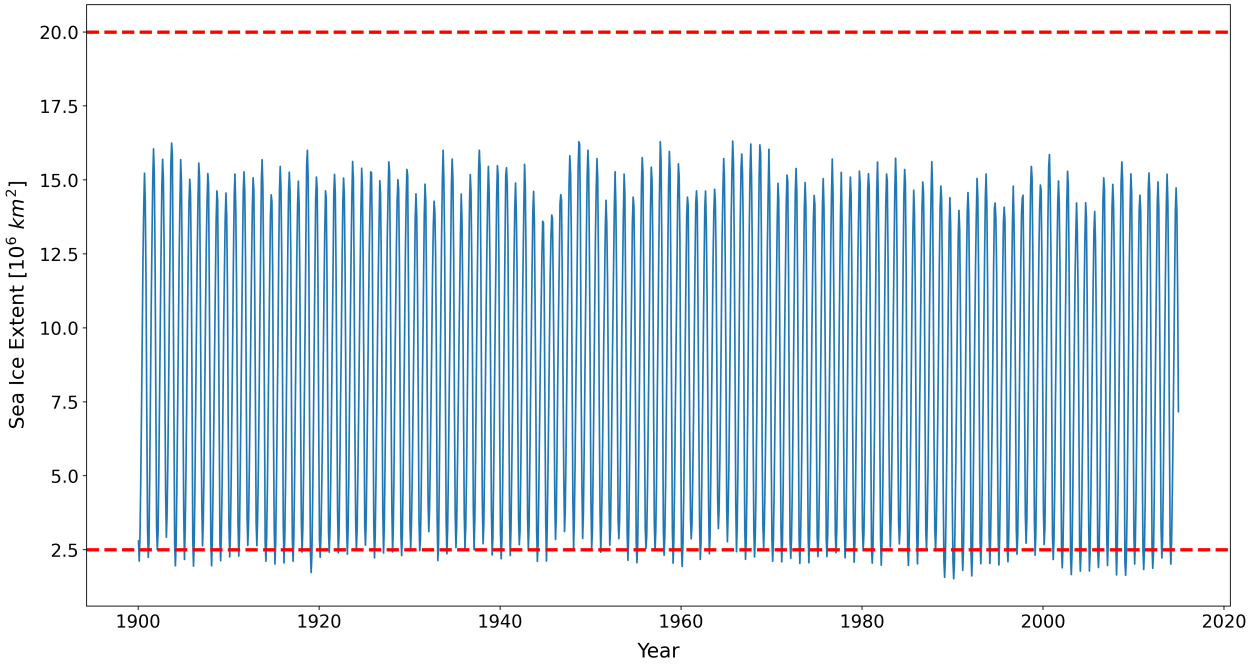

Figure 31: Annual sea ice extent seasonal cycle time series for the previous century, produced by climate model NorESM2-MM. Red lines demarcate sea ice extent seasonal minimum and maximum based on previous literature (See Section 2.2.2).

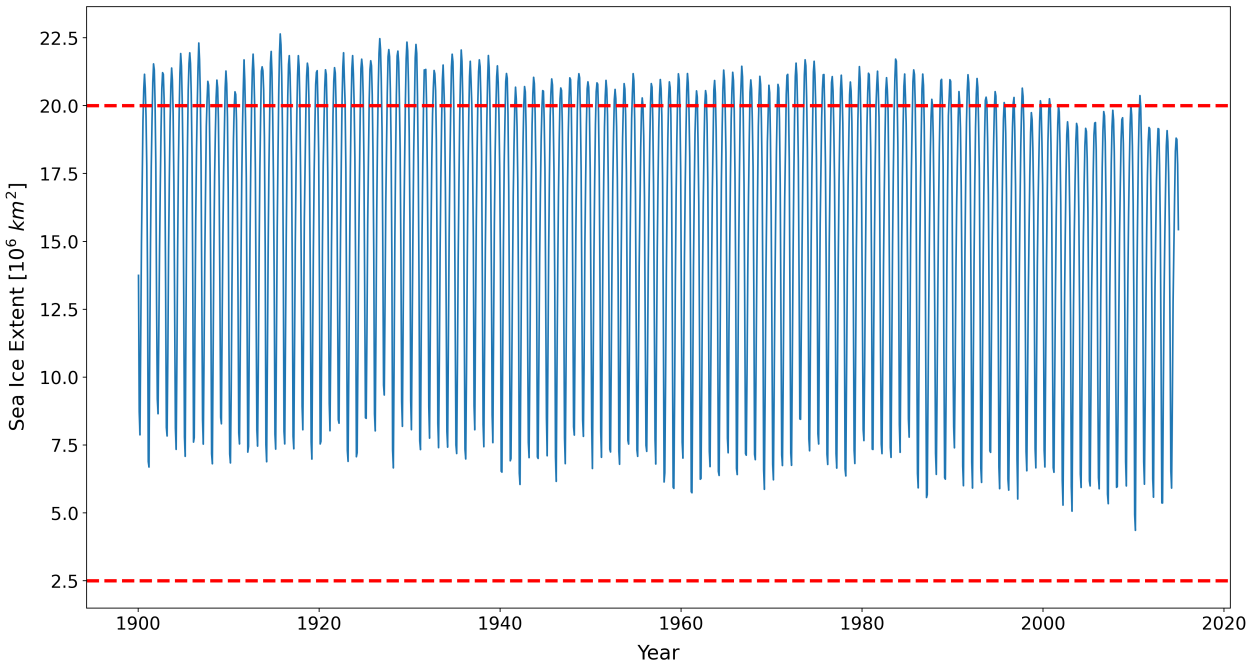

Figure 32: Annual sea ice extent seasonal cycle time series for the previous century, produced by climate model SAM0-UNICON. Red lines demarcate sea ice extent seasonal minimum and maximum based on previous literature (See Section 2.2.2).

References

N Abram, J.P Gattuso, A Prakash, L Cheng, M.P Chidichimo, S Crate, H Enomoto, M Garschagen, N Gruber, S Harper, E Holland, R.M Kudela, J Rice, K Steffen, and K von Schuckmann. IPCC special report on the ocean and cryosphere in a changing climate. 2019.

A Adcroft, W Anderson, V Balaji, C Blanton, M Bushuk, C.O Dufour, J.P Dunne, S.M Griffies, R Hallberg, M.J Harrison, I.M Held, M.F Jansen, J.G John, J.P Krasting, A.R Langenhorst, S Legg, Z Liang, C McHugh, A Radhakrishnan, B.G Reichl, T Rosati, B.L Samuels, A Shao, R Stouffer, M Winton, A.T Wittenberg, B Xiang, N Zadeh, and R Zhang. The GFDL global ocean and sea ice model OM4.0: Model description and simulation features. *Journal of Advances in Modeling Earth Systems*, 11(10):3167–3211, 2019. doi: 10.1029/2019MS001726.

G.R Albertson, A.S Friedlaender, D.J Steel, A Aguayo-Lobo, S.L Bonatto, S Caballero, R Constantine, A.L Cypriano-Souza, M.H Engel, C Garrigue, et al. Temporal stability and mixed-stock analyses of humpback whales (Megaptera novaeangliae) in the nearshore waters of the Western Antarctic Peninsula. *Polar Biology*, 41(2):323–340, 2018.

AR Amaral, J Loo, H Jaris, C Olavarria, D Thiele, P Ensor, A Aguayo, and HC Rosenbaum. Population genetic structure among feeding aggregations of humpback whales in the Southern Ocean. *Marine biology*, 163(6):132, 2016.

V Andrews, S Bestley, N.J Gales, S.M Laverick, D Paton, A.M Polanowski, N.T Schmitt, and M.C Double. Humpback whale migrations to Antarctic summer foraging grounds through the southwest Pacific Ocean. *Scientific Reports*, 8, 2018. doi: 10.1038/s41598-018-30748-4.

A Atkinson, V Siegel, E Pakhomov, and P Rothery. Long-term decline in krill stock and increase in salps within the Southern Ocean. *Nature*, 432(7013):100–103, 2004.

R.W Baird. *International Geophysical Year*, pages 608–611. Springer Netherlands, 2011. doi: 10.1007/978-90-481-8702-7_237.

M Bentsen, D.J.L Oliviè, Ø Seland, T Toniazzo, A Gjermundsen, L.S Graff, J.B Debernard, A.K Gupta, Y He, A Kirkevåg, J Schwinger, J Tjiputra, K.S Aas, I Bethke, Y Fan, J Griesfeller, A Grini, C Guo, M Ilicak, I.H.H Karset, O.A Landgren, J Liakka, K.O Moseid, A Nummelin, C Spensberger, H Tang, Z Zhang, C Heinze, T Iversen, and M Schulz. NCC NorESM2-MM model output prepared for CMIP6 CMIP historical, 2019.

I Bethke, Y Wang, F Counillon, M Kimmritz, F Fransner, A Samuelsen, H.R Langehaug, P-G Chiu, M Bentsen, C Guo, J Tjiputra, A Kirkevåg, D.J.L Oliviè, Ø Seland, Y Fan, P Lawrence, T Eldevik, and N Keenlyside. NCC NorCPM1 model output prepared for CMIP6 CMIP historical, 2019.

G.A Bortolotto, D Danilewicz, P.S Hammond, L Thomas, and A.N Zerbini. Whale distribution in a breeding area: spatial models of habitat use and abundance of western South Atlantic humpback whales. *Marine Ecology Progress Series*, 585:213–227, 2017.

O Boucher, S Denvil, A Caubel, and M.A Foujols. IPSL IPSL-CM6A-LR model output prepared for CMIP6 CMIP historical, 2018.

L Dalla Rosa, E.R Secchi, YG Maia, AN Zerbini, and MP Heide-Jørgensen. Movements of satellite-monitored humpback whales on their feeding ground along the Antarctic peninsula. *Polar Biology*, 31(7):771–781, 2008.

G Danabasoglu. NCAR CESM2 model output prepared for CMIP6 CMIP historical, 2019.

W.K de la Mare. Abrupt mid-twentieth-century decline in Antarctic sea-ice extent from whaling records. *Nature*, 389(6646):57–60, 1997.

W.K de la Mare. Changes in Antarctic sea-ice extent from direct historical observations and whaling records. *Climatic Change*, 92(3-4):461–493, 2009.

M Dix, D Bi, P Dobrohotoff, R Fiedler, I Harman, R Law, C Mackallah, S Marsland, S O'Farrell, H Rashid, J Srbinovsky, A Sullivan, C Trenham, P Vohralik, I Watterson, G Williams, M Woodhouse, R Bodman, F.B Dias, C Domingues, N Hannah, A Heerdegen, A Savita, S Wales, C Allen, K Druken, B Evans, C Richards, S.M Ridzwan, D Roberts, J Smillie, K Snow, M Ward, and R Yang. CSIRO-ARCCSS ACCESS-CM2 model output prepared for CMIP6 CMIP historical, 2019.

C Eayrs, D Holland, D Francis, T Wagner, R Kumar, and X Li. Understanding the seasonal cycle of Antarctic sea ice extent in the context of longer-term variability. *Reviews of Geophysics*, 57(3):1037–1064, 2019. doi: 10.1029/2018RG000631.

EC-Earth Consortium (EC-Earth). EC-Earth-Consortium EC-Earth3 model output prepared for CMIP6 CMIP historical, 2019.

K.P Findlay, S.M Seakamela, M.A Meÿer, S.P Kirkman, J Barendse, D.E Cade, D Hurwitz, A.S. Kennedy, P.G.H Kotze, S.A McCue, M Thornton, O.A Vargas-Fonseca, and C.G Wilke. Humpback whale âsupergroupsâ â A novel low-latitude feeding behaviour of Southern Hemisphere humpback whales (Megaptera novaeangliae) in the Benguela Upwelling System. *PLOS ONE*, 12(3):1–18, 2017. doi: 10.1371/journal.pone.0172002.

G Flato, J Marotzke, B Abiodun, P Braconnot, S.C Chou, W Collins, P Cox, F Driouech, S Emori, V Eyring, et al. Evaluation of climate models. In *Climate change 2013: the physical science basis. Contribution of Working Group I to the Fifth Assessment Report of the Intergovernmental Panel on Climate Change*, pages 741–866. Cambridge University Press, 2014.

A.S Friedlaender, P.N Halpin, S Qian, G.L Lawson, P.H Wiebe, D Thiele, and A.J Read. Whale distribution in relation to prey abundance and oceanographic processes in shelf waters of the Western Antarctic Peninsula. *Marine Ecology Progress Series*, 317:297–310, 2006.

A.S Friedlaender, G.L Lawson, and P.N Halpin. Evidence of resource partitioning between humpback and minke whales around the Western Antarctic Peninsula. *Marine mammal science*, 25(2):402–415, 2009.

Greenpeace. Defending the whales whaling timeline. Technical report, Greenpeace.

H Guo, J.G John, C Blanton, C McHugh, S Nikonov, A Radhakrishnan, K Rand, N.T Zadeh, V Balaji, J Durachta, C Dupuis, R Menzel, T Robinson, S Underwood, H Vahlenkamp, M Bushuk, K.A Dunne, R Dussin, P.P.G Gauthier, P Ginoux, S.M Griffies, R Hallberg, M Harrison, W Hurlin, S Malyshev, V Naik, F Paulot, D.J Paynter, J Ploshay, B.G Reichl, D.M Schwarzkopf, C.J Seman, A Shao, L Silvers,

B Wyman, X Yan, Y Zeng, A Adcroft, J.P Dunne, I.M Held, J.P Krasting, L.W Horowitz, P.C.D Milly, E Shevliakova, M Winton, M Zhao, and R Zhang. NOAA-GFDL GFDL-CM4 model output historical, 2018.

F.A Haumann, D Notz, and H Schmidt. Anthropogenic influence on recent circulation-driven Antarctic sea ice changes. *Geophysical Research Letters*, 41(23):8429–8437, 2014. doi: 10.1002/2014GL061659.

F.A Haumann, N Gruber, and M Münnich. Sea-ice induced Southern Ocean subsurface warming and surface cooling in a warming climate. *AGU Advances*, 1(2), 2020. doi: 10.1029/2019av000132.

Z Hausfather. CMIP6: the next generation of climate models explained. 2019.

B He, Y Liu, G Wu, Q Bao, T Zhou, X Wu, W Lei, J Li, X Wang, J Li, W Hu, X Zhang, C Sheng, and T Yiqiong. CAS FGOALS-f3-L model datasets for CMIP6 GMMIP tier-1 and tier-3 experiments. *Advances in Atmospheric Sciences*, 37:18–28, 2020. doi: 10.1007/s00376-019-9085-y.

I Held, H Guo, A Adcroft, J Dunne, L Horowitz, J Krasting, E Shevliakova, M Winton, M Zhao, M Bushuk, A Wittenberg, B Wyman, B Xiang, R Zhang, W Anderson, V Balaji, L Donner, K Dunne, J Durachta, and N Zadeh. Structure and performance of GFDL's CM4.0 climate model. *Journal of Advances in Modeling Earth Systems*, 11:3691–3727, 2019. doi: 10.1029/2019MS001829.

W.R Hobbs, R Massom, S Stammerjohn, P Reid, G Williams, and W Meier. A review of recent changes in Southern Ocean sea ice, their drivers and forcings. *Global and Planetary Change*, 143:228–250, 2016.

T Ichii. Distribution of Antarctic krill concentrations exploited by Japanese krill trawlers and minke whales. *Proceedings of the NIPR Symposium on Polar Biology*, 3:36–56, 1990.

J Jungclaus, M Bittner, K-H Wieners, F Wachsmann, M Schupfner, S Legutke, M Giorgetta, C Reick, V Gayler, H Haak, P de Vrese, T Raddatz, M Esch, T Mauritsen, J-S von Storch, J Behrens, V Brovkin, M Claussen, T Crueger, I Fast, S Fiedler, S Hagemann, C Hohenegger, T Jahns, Kloster, S Kinne, G Lasslop, L Kornblueh, J Marotzke, D Matei, K Meraner, U Mikolajewicz, K Modali, W Müller, J Nabel, D Notz, K Peters, R Pincus, H Pohlmann, J Pongratz, S Rast, H Schmidt, R Schnur, U Schulzweida, K Six, B Stevens, A Voigt, and E Roeckner. MPI-M MPI-ESM1.2-HR model output prepared for CMIP6 CMIP historical, 2019.

J.P Krasting, J.G John, C Blanton, C McHugh, S Nikonov, A Radhakrishnan, K Rand, N.T Zadeh, V Balaji, J Durachta, C Dupuis, R Menzel, T Robinson, S Underwood, H Vahlenkamp, K.A Dunne, P.P.G Gauthier, P Ginoux, S.M Griffies, R Hallberg, M Harrison, W Hurlin, S Malyshev, V Naik, F Paulot, D.J Paynter, J Ploshay, D.M Schwarzkopf, C.J Seman, L Silvers, B Wyman, Y Zeng, A Adcroft, J.P Dunne, R Dussin, H Guo, J He, I.M Held, L.W Horowitz, P Lin, P.C.D Milly, E Shevliakova, C Stock, M Winton, Y Xie, and M Zhao. NOAA-GFDL GFDL-ESM4 model output prepared for CMIP6 CMIP historical, 2018.

M Krzywinski and N Altman. Visualizing samples with box plots. *nature methods*, 11(2), 2014.

T Lavergne, A. M Sørensen, S Kern, R Tonboe, D Notz, S Aaboe, L Bell, G Dybkjær, S Eastwood, C Gabarro, G Heygster, M. A Killie, M Brandt Kreiner, J Lavelle, R. Saldo, S. Sandven, and L. T. Pedersen. Version 2 of the EUMETSAT OSI SAF and ESA CCI sea-ice concentration climate data records. *The Cryosphere*, 13(1):49–78, 2019. doi: 10.5194/tc-13-49-2019.

T.J Lavery, B Roudnew, P Gill, J Seymour, L Seuront, G Johnson, J.G Mitchell, and V Smetacek. Iron defecation by sperm whales stimulates carbon export in the Southern Ocean. *Proceedings: Biological Sciences*, 277(1699):3527–3531, 2010.

W-L Lee and H-C Liang. AS-RCEC TaiESM1.0 model output prepared for CMIP6 CMIP historical, 2020.

L Li. CAS FGOALS-g3 model output prepared for CMIP6 CMIP historical, 2019.

R.A Massom and S.E Stammerjohn. Antarctic sea ice change and variability–physical and ecological implications. *Polar Science*, 4(2):149–186, 2010.

T Mauritsen, J Bader, T Becker, J Behrens, M Bittner, R Brokopf, V Brovkin, M Claussen, T Crueger, M Esch, I Fast, S Fiedler, D Fläschner, V Gayler, M Giorgetta, D.S Goll, H Haak, S Hagemann, C Hedemann, C Hohenegger, T Ilyina, T Jahns, D Jimenéz-de-la Cuesta, J Jungclaus, T Kleinen, S Kloster, D Kracher, S Kinne, D Kleberg, G Lasslop, L Kornblueh, J Marotzke, D Matei, K Meraner, U Mikolajewicz, K Modali, B Möbis, W.A Müller, J.E.M.S Nabel, C.C.W Nam, D Notz, S-S Nyawira, H Paulsen, K Peters, R Pincus, H Pohlmann, J Pongratz, M Popp, T.J Raddatz, S Rast, R Redler, C.H Reick, T Rohrschneider, V Schemann, H Schmidt, R Schnur, U Schulzweida, K.D Six, L Stein, I Stemmler, B Stevens, J-S von Storch, F Tian, A Voigt, P Vrese, K-H Wieners, S Wilkenskjeld, A Winkler, and E Roeckner. Developments in the MPI-M Earth System Model version 1.2 (MPI-ESM1.2) and its response to increasing co2. *Journal of Advances in Modeling Earth Systems*, 11(4):998–1038, 2019. doi: 10.1029/2018MS001400.

M Mcbride, P Dalpadado, K Drinkwater, O Godø, A Hobday, A Hollowed, T Kristiansen, E Murphy, P Ressler, S Subbey, E Hofmann, and H Loeng. Krill, climate, and contrasting future scenarios for Arctic and Antarctic fisheries. *ICES Journal of Marine Science*, 71:1934–1955, 2014. doi: 10.1093/icesjms/fsu002.

A.J.S Meijers. The Southern Ocean in the coupled model intercomparison project phase 5. *Philosophical Transactions of the Royal Society A: Mathematical, Physical and Engineering Sciences*, 372(2019): 20130296, 2014.

J-O Meynecke, E Seyboth, J De Bie, J-K Menzel Barraqueta, A Chama, S Prakash Dey, S.B Lee, V Tulloch, M Vichi, K Findlay, A.N Roychoudhury, and B Mackey. Responses of humpback whales to a changing climate in the Southern Hemisphere: Priorities for research efforts. *Marine Ecology*. doi: 10.1111/maec.12616.

H Murase, K Matsuoka, T Ichii, and S Nishiwaki. Relationship between the distribution of euphausiids and baleen whales in the Antarctic (35 E–145 W). *Polar Biology*, 25(2):135–145, 2002.

D Neubauer, S Ferrachat, C Siegenthaler-Le Drian, J Stoll, D.S Folini, I Tegen, K-H Wieners, T Mauritsen, I Stemmler, S Barthel, I Bey, N Daskalakis, B Heinold, H Kokkola, D Partridge, S Rast, H Schmidt, N Schutgens, T Stanelle, P Stier, D Watson-Parris, and U Lohmann. HAMMOZ-Consortium MPI-ESM1.2-HAM model output prepared for CMIP6 CMIP historical, 2019.

S.V Nghiem, I.G Rigor, P Clemente-Colón, G Neumann, and P.P Li. Geophysical constraints on the Antarctic sea ice cover. *Remote Sensing of Environment*, 181:281 – 292, 2016. doi: https://doi.org/10.1016/j.rse.2016.04.005.

S Nicol, T Pauly, N.L Bindoff, S Wright, D Thiele, G.W Hosie, P.G Strutton, and E Woehler. Ocean circulation off east Antarctica affects ecosystem structure and sea-ice extent. *Nature*, 406(6795):504–507, 2000.

D Notz, A Jahn, M Holland, E Hunke, F Massonnet, J Stroeve, B Tremblay, and M Vancoppenolle. The CMIP6 Sea-Ice Model Intercomparison Project (SIMIP): understanding sea ice through climate-model simulations. *Geoscientific Model Development (Online)*, 9(LA-UR-16-25878), 2016.

S Park and J Shin. SNU SAM0-UNICON model output prepared for CMIP6 CMIP historical, 2019.

A.J Pershing, L.B Christensen, N.R Record, G.D Sherwood, and P.B Stetson. The impact of whaling on the ocean carbon cycle: Why bigger was better. *PLoS ONE*, 5(8):1–9, 2010. doi: 10.1371/journal.pone.0012444.

E.S Poloczanska, C.J Brown, W.J Sydeman, W Kiessling, D.S Schoeman, P.J Moore, K Brander, J.F Bruno, L.B Buckley, M.T Burrows, C.M Duarte, B.S Halpern, J Holding, C.V Kappel, M.I OâConnor, J.M Pandolfi, C Parmesan, F Schwing, S-A Thompson, and A.J Richardson. Global imprint of climate change on marine life. *Nature Climate Change*, 3:919–925, 2013. doi: https://doi-org.ezproxy.uct.ac.za/10.1038/nclimate1958.

C Ramp, J Delarue, P.J Palsbøll, R Sears, and P.S Hammond. Adapting to a warmer ocean - Seasonal shift of baleen whale movements over three decades. *PLoS ONE*, 10(3):1–15, 2015. doi: 10.1371/journal.pone.0121374.

K Rasmussen, D.M Palacios, J Calambokidis, M.T Saborío, L Dalla Rosa, E.R Secchi, G.H Steiger, J.M Allen, and G.S Stone. Southern Hemisphere humpback whales wintering off Central America: insights from water temperature into the longest mammalian migration. *Biology Letters*, 3(3):302–305, 2007. doi: 10.1098/rsbl.2007.0067.

R Revelle and H.E Suess. Carbon dioxide exchange between atmosphere and ocean and the question of an increase of atmospheric co2 during the past decades. *Tellus*, 9(1):18–27, 1957. doi: 10.1111/j.2153-3490.1957.tb01849.x.

L.A Roach, S.M Dean, and J.A Renwick. Consistent biases in Antarctic sea ice concentration simulated by climate models. *The Cryosphere*, 12:365–383, 2018. doi: https://doi.org/10.5194/tc-12-365-2018.

X Rong. CAMS $CAMS_CSM1.0model output prepared for CMIP6 CMIP historical$, 2019.

J.L Russell, I Kamenkovich, C Bitz, R Ferrari, S.T Gille, P.J Goodman, R Hallberg, K Johnson, K Khazmutdinova, I Marinov, et al. Metrics for the evaluation of the Southern Ocean in coupled climate models and earth system models. *Journal of Geophysical Research: Oceans*, 123(5):3120–3143, 2018.

J.B Sallée. Southern Ocean warming. *Oceanography*, 2018.

J.A Santora, C.S Reiss, V.J Loeb, and R.R Veit. Spatial association between hotspots of baleen whales and demographic patterns of Antarctic krill euphausia superba suggests size-dependent predation. *Marine Ecology Progress Series*, 405:255–269, 2010.

Ø Seland, M Bentsen, D.J.L Oliviè, T Toniazzo, A Gjermundsen, L.S Graff, J.B Debernard, A.K Gupta, Y He, A Kirkevåg, J Schwinger, J Tjiputra, K.S Aas, I Bethke, Y Fan, J Griesfeller, A Grini, C Guo, M Ilicak, I.H.H Karset, O.A Landgren, J Liakka, K.O Moseid, A Nummelin, C Spensberger, H Tang, Z Zhang, C Heinze, T Iversen, and M Schulz. NCC NorESM2-LM model output prepared for CMIP6 CMIP historical, 2019.

G Smith. The international whaling commission: An analysis of the past and reflections on the future. *Natural Resources Lawyer*, 16(4):543–567, 1984.

S Sokolov and S.R Rintoul. On the relationship between fronts of the Antarctic Circumpolar Current and surface chlorophyll concentrations in the Southern Ocean. *Journal of Geophysical Research: Oceans*, 112 (C7), 2007.

Z Song, F Qiao, Y Bao, Q Shu, Y Song, and X Yang. FIO-QLNM FIO-ESM2.0 model output prepared for CMIP6 CMIP historical, 2019.

P.T Stevick, M.C Neves, F Johansen, M.H Engel, J Allen, M.C.C Marcondes, and C Carlson. A quarter of a world away: female humpback whale moves 10 000 km between breeding areas. *Biology Letters*, 7: 299–302, 2011. doi: https://doi.org/10.1098/rsbl.2010.0717.

S Surma, E.A Pakhomov, and T.J Pitcher. Effects of whaling on the structure of the Southern Ocean food web: insights on the âKrill Surplusâ from ecosystem modelling. *PLoS One*, 9(12), 2014.

N.C Swart, J.N.S Cole, V.V Kharin, M Lazare, J.F Scinocca, N.P Gillett, J Anstey, V Arora, J.R. Christian, Y Jiao, W.G Lee, F Majaess, O.A Saenko, C Seiler, C Seinen, A Shao, L Solheim, K von Salzen, D Yang, B Winter, and M Sigmond. CCCma CanESM5 model output prepared for CMIP6 CMIP historical, 2019.

L.D Talley. *Descriptive physical oceanography: an introduction*. Academic press, 2011.

H Tatebe and M Watanabe. MIROC MIROC6 model output prepared for CMIP6 CMIP historical, 2018.

R Tonboe, J Lavelle, H Pfeiffer, and E Howe. Ocean & sea ice SAF: Product user manual for OSI SAF global sea ice concentration. Technical Report September, 2017.

V.J.D Tulloch, É.E. Plagányi, C Brown, A.J Richardson, and R Matear. Future recovery of baleen whales is imperiled by climate change. *Global Change Biology*, 25(4):1263–1281, 2019. doi: 10.1111/gcb.14573.

B van Drimmelen. Pacific basin law journal. *Pacific Basin Law Journal*, (13 (2)):231–264, 1995.

D Veytia, S Corney, K.M Meiners, S Kawaguchi, E.J Murphy, and S Bestley. Circumpolar projections of Antarctic krill growth potential. *Nature Climate Change*, 10:568–575, 2020. doi: https://doi.org/10.1038/s41558-020-0758-4.

V.M Walsh. Illegal whaling for humpbacks by the Soviet Union in the Antarctic, 1947-1972. *The Journal of Environment Development*, 8(3):307–327, 1999.

K-H Wieners, M Giorgetta, J Jungclaus, C Reick, M Esch, M Bittner, S Legutke, M Schupfner, F Wachsmann, V Gayler, H Haak, P de Vrese, T Raddatz, T Mauritsen, J-S von Storch, J Behrens, V Brovkin, M Claussen, T Crueger, I Fast, S Fiedler, S Hagemann, C Hohenegger, T Jahns, S Kloster, S Kinne, G Lasslop, L Kornblueh, J Marotzke, D Matei, K Meraner, U Mikolajewicz, K Modali, W Müller, J Nabel,

D Notz, K Peters, R Pincus, H Pohlmann, J Pongratz, S Rast, H Schmidt, R Schnur, U Schulzweida, K Six, B Stevens, A Voigt, and E Roeckner. MPI-M MPI-ESM1.2-LR model output prepared for CMIP6 CMIP historical, 2019.

WWF. The history of whaling and the International Whaling Commission. (June):1–5, 2009.

Y Yu. CAS FGOALS-f3-L model output prepared for CMIP6 CMIP historical, 2019.

S Yukimoto, T Koshiro, H Kawai, N Oshima, K Yoshida, S Urakawa, H Tsujino, M Deushi, T Tanaka, M Hosaka, H Yoshimura, E Shindo, R Mizuta, M Ishii, A Obata, and Y Adachi. MRI MRI-ESM2.0 model output prepared for CMIP6 CMIP historical, 2019.

T Ziehn, M Chamberlain, A Lenton, R Law, R Bodman, M Dix, Y Wang, P Dobrohotoff, J Srbinovsky, L Stevens, P Vohralik, C Mackallah, A Sullivan, S O'Farrell, and K Druken. CSIRO ACCESS-ESM1.5 model output prepared for CMIP6 CMIP historical, 2019.

V Zunz, H Goosse, and F Massonnet. How does internal variability influence the ability of CMIP5 models to reproduce the recent trend in Southern Ocean sea ice extent? *The Cryosphere*, 7(2):451, 2013.